Wideband Modulation and Tuning of Semiconductor Lasers using Novel Quantum Well Structures

Special Contract SPC-93-4072

First Year Report

prepared by

Xuan Huang and Alwyn Seeds

Department of Electronic and Electrical Engineering,
University College London
Torrington Place, London, WC1E 7JE.

Tel.: +44 171 380 7928, FAX: +44 171 388 9325, e-mail: a.seeds@eleceng.ucl.ac.uk

REPORT DOCUMENTATION PAGE

Form Approved OMB No. 0704-0188

1. AGENCY USE ONLY (Leave blank)	2. REPORT DATE	3. REPORT TYPE AND DATES COVERED
	1994	Final Report

4. TITLE AND SUBTITLE

Wideband Modulation and Tuning of Semiconductor Lasers using Novel Quantum Well Structures

5. FUNDING NUMBERS

Unknown

6. AUTHOR(S)

Xuan Huang and Alwyn Seeds

7. PERFORMING ORGANIZATION NAME(S) AND ADDRESS(ES)

Department of Electronic and Electrical Engineering
University College London
Torrington Place, London WC1E 7JE

8. PERFORMING ORGANIZATION REPORT NUMBER

SPC-93-4072

9. SPONSORING/MONITORING AGENCY NAME(S) AND ADDRESS(ES)

EOARD
PSC 802 BOX 14
FPO AE 09499-0200

10. SPONSORING/MONITORING AGENCY REPORT NUMBER

SPC-93-4079

11. SUPPLEMENTARY NOTES

12a. DISTRIBUTION/AVAILABILITY STATEMENT

Approved for public release; distribution is unlimited.

12b. DISTRIBUTION CODE

A

13. ABSTRACT (Maximum 200 words)

14. SUBJECT TERMS

EOARD

15. NUMBER OF PAGES

67

16. PRICE CODE

N/A

17. SECURITY CLASSIFICATION OF REPORT	18. SECURITY CLASSIFICATION OF THIS PAGE	19. SECURITY CLASSIFICATION OF ABSTRACT	20. LIMITATION OF ABSTRACT
UNCLASSIFIED	UNCLASSIFIED	UNCLASSIFIED	UL

NSN 7540-01-280-5500

Standard Form 298 (Rev. 2-89)
Prescribed by ANSI Std. 239-18
298-102

Abstract

Angle modulation techniques enable analogue optical transmission systems to be realised which have dynamic ranges in excess of those possible with conventional intensity modulation direct detection (IMDD) links. Tunable semiconductor lasers are essential components for links employing optical frequency modulation (OFM) for enhanced dynamic range or dense wavelength division multiplex (DWDM) for multi-channel capability. They are also key components in many advanced sensor systems. Existing lasers use the forward bias carrier injection effect (CIE) to achieve tuning. Whilst this is a convenient technique for wavelength setting it suffers from severe limitations when fast tuning or modulation of the laser frequency is required. At low modulation frequencies the response is dominated by thermal effects, leading to a decrease in emission frequency with increasing current, whereas at high frequencies the response is dominated by plasma and band filling effects giving an increase in frequency with increasing current. The resulting overall frequency response typically varies by more than an order of magnitude from 0-1GHz accompanied by phase variations of up to π radians. Equalising such a response, even over a restricted frequency range, requires complex networks that have to be optimised for the particular laser and its operating conditions. Improved uniformity of response has been obtained in multi-electrode distributed feedback (DFB) lasers by carefully adjusting the distribution of current between sections, but the high frequency response tends to be limited by carrier lifetime in the section biased below transparency to about 1GHz.

In earlier work we demonstrated, for the first time, a novel semiconductor laser tuning technique using the refractive index change in reverse biased multiple quantum well (MQW) PIN structures. The technique was used in an external cavity laser system to demonstrate a tuning response that was uniform to within ±1.6dB from 30 kHz to 1.3 GHz, the upper frequency limit being set by the parasitic capacitance of the tuning element. This laser has been used as the source in an optical FM link demonstrator.

External cavity lasers are mechanically sensitive and unsuitable for use in production systems; the tuning speed is also limited by round-trip time effects in the necessarily long optical cavity. A logical development is therefore to integrate the laser gain section and tuning element monolithically. The objective of work under this Special Contract is to develop fabrication techniques for a monolithically integrated reverse bias tuned semiconductor laser and to assess its performance. In this report we describe the work carried out in the first year of the Contract. Specific technical accomplishments in this first year include the design of the MQW laser and tuning element structure, the development of fabrication techniques for successful realisation of a two-section ridge guide laser, the fabrication of two section ridge guide lasers capable of room temperature CW operation and having CW threshold currents as low as 25 mA and output powers greater than 10 mW, the achievement of single longitudinal mode (SLM) operation and the detailed assessment of laser operation.

1. Introduction and Historical Review

Tunable lasers are essential components in advanced optical communication systems, including multi-channel systems for multiple antenna remoting and CATV distribution[1], and in dense wavelength division multiplex (DWDM) optical networks[2-4] which are likely to become the fourth generation of optical fibre communication systems.[5] Compared to the first generation system which employed 850 nm semiconductor lasers, the second generation system which used 1.3 μm laser, and the third generation system which is based on the 1.55 μm laser, the coherent optical communication system offers better transmission quality and much higher information density.[6,7] In this system, the tunable laser is the key device.[8] In the early stage of coherent optical communication system research, gas lasers were used to demonstrate the basic principles of system operation.[9] Considering their size and reliability, it is almost impossible to operate such a system outside a laboratory environment. Of the source technologies available currently, the semiconductor laser is the most promising one, due to its small size, mechanical stability and potential for volume manufacture. Development of high performance tunable semiconductor lasers is thus of much interest. The purpose of this project is to study and develop a new kind of tunable laser to meet some key requirements of coherent systems.

In spite of the variety of coherent communication schemes proposed,[10-14] some common requirements are put forward for tunable lasers. A good tunable laser for such systems should be single mode with narrow spectral linewidth, fast modulation response speed and uniform frequency modulation response. Depending on the coherent system adopted, different specific performance parameters are required. For use in wavelength/frequency division multiplexing, a large tuning range is desirable(several 1000's GHz), although the range could be the combination of a series of large separated discontinuous tuning bands each with a small range of continuous tuning. On the other hand, for optical frequency modulation (OFM) applications only a few gigahertz tuning range is demanded, but fast tuning speed, continuous tuning range and flat frequency modulation response become the critical requirements.

In our earlier work, a novel semiconductor laser tuning technique using refractive index change by the quantum-confined Stark effect (QCSE) in reverse biased multi quantum well (MQW) p-i-n structures was demonstrated for the first time.[15,16] The technique was used in an external cavity laser system, and the frequency modulation response(FMR) was found to be uniform to within ± 1.6 dB from 30kHz-1.3GHz with the upper frequency limit set by the parasitic parameters of the device, not the tuning mechanism itself.[16] The advantages of fast tuning speed and uniform FM response are highly attractive for OFM and similar applications. As external cavity lasers are mechanically sensitive and unsuitable for use in practical systems, a logical progression is to develop a monolithically integrated tunable laser utilising the same principles.

Most of the early tunable semiconductor lasers were associated with the attempts to achieve single longitudinal mode and narrow linewidth operation of semiconductor lasers, which at that time

normally operated in multiple longitudinal modes, and the reduction of linewidth was limited by the intrinsic nature of spontaneous emission noise and relatively high cavity loss.[17-19] By increasing the laser cavity length via either using a long laser chip or extending the cavity with a passive medium such as air, an optical fibre or a passive waveguide, the linewidth can be reduced. The latter external cavity devices also provided mode selectivity or mode shift to allow single longitudinal mode (SLM) operation with tunability of wavelength/frequency.

In this report, a historical review of tunable lasers will be presented; the principles, design and fabrication processes of the reverse biased, monolithically integrated two section tunable laser will be described, the experimental results so far will be given and, finally, further research work will be outlined.

1.1. Tunable external cavity lasers

There are three main approaches to external cavity tunable semiconductor lasers; the grating external cavity laser, the electro-optic birefringent external cavity laser and the acoustic-optic external cavity laser.

1.1.1. Grating external cavity tunable laser

The grating external cavity tunable laser, as shown in Fig.1.1, was first introduced by Edmonds and Smith in 1970.[20] In their experiment, the oscillation of the internal modes was prevented by an anti-reflection (AR) coated facet on one of the two cleaved surfaces in the Fabry-Perot cavity semiconductor laser. The actual resonator was formed by the external grating and the other facet of the semiconductor laser. By rotating the grating, the diffraction wavelength coupled into the semiconductor cavity through the AR coated facet was changed, therefore changing the oscillation wavelength in the composite cavity, and wavelength tuning was obtained. Note that as the tuning involved only the selection of the oscillation modes defined by the resonator of the semiconductor facet/external grating cavity, the tuning certainly was discontinuous. Due to the long external cavity and the mode selectivity of the grating, the device had a small mode spacing, single longitudinal mode operation and small linewidth.

In another similar experiment carried out by Thomas[21], there was no AR coating on the semiconductor laser facets, therefore the internal oscillation modes of the semiconductor laser were selected by the external grating. The tuning was discontinuous and with larger mode spacing because of the shorter semiconductor cavity than the above experiment.

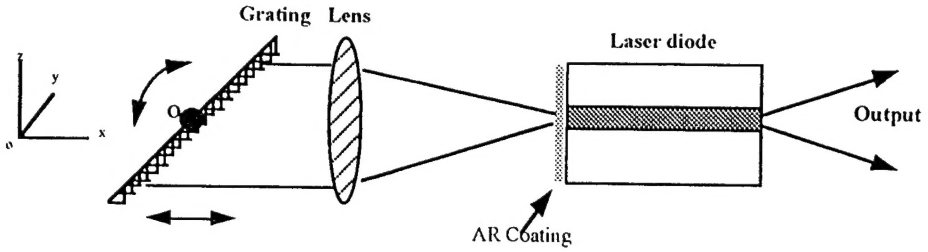

Fig. 1. 1 Grating external cavity laser.

In both experiments, the grating acted as a mode selecting, rather than mode shifting, element so that only discontinuous tuning is available. In order to achieve continuous tuning, mode shifting mechanisms or optical length change in the cavity must be introduced.

Based on this idea, a continuous tuning device was developed,[22] which incorporated grating rotation round its own centre axis **Y** and the grating lateral translation along X axis as shown in Fig.1.1. The translation along X axis changed the resonator length, therefore changed the optical length, and the oscillating wavelength was continuously shifted accordingly. By carefully mechanical design, it is possible to match the continuous mode shifting caused by optical length changing and the discontinuous mode selection caused by grating rotation, to achieve a large range of continuous tuning.[22]

Another approach to the long external cavity tunable laser employed an external prism and graded-index (GRIN) rod lens[23] combined with one facet AR coated semiconductor lasers,[24,25] as shown in Fig.1.3. This technique enabled coarse wavelength adjustment of a buried heterostructure single mode laser over a range of 40 nm through lateral displacement of the GRIN rod lens relative to the laser chip so changing the oscillating mode coupled into the laser by selecting the refraction wavelength from prism grating. Fine tuning of around 6 GHz/mm could be achieved by slight variations in the separation between the laser facet and the GRIN rod lens end face which changed the oscillator cavity length

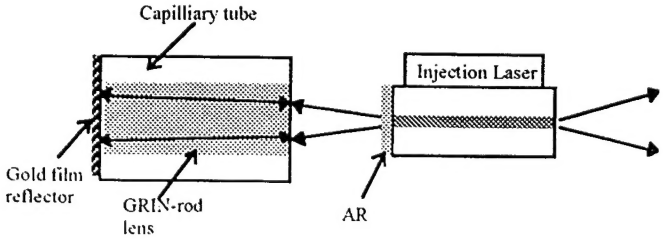

Fig. 1. 2 External cavity laser using GRIN-rod lens.

The advantages of this grating external cavity laser are that the tuning range could be very large. Tuning ranges of over 105nm in GaAs/AlGaAs[26] and 160nm in InGaAsP/InP[27] quantum well

lasers with external grating cavities have been demonstrated. Also the spectral linewidth could be very narrow (< 1MHz)[28,29] due to the long optical cavity, and the single longitudinal mode operation is easily realised by the mode selectivity of the grating. The principle disadvantages of these mechanically tuned devices are their mechanical instability and the need for precise adjustment as the long optical cavity provides very small mode spacing, together with their low switching/response speed (typically 1ms) due to the dependence on mechanical movement of tuning elements. They are obviously difficult to use in a practical system. However, they are quite useful in testing more advanced tuning schemes or in laboratory environments.

Much higher tuning speed can be achieved by using electro-optic or acousto-optic devices as the tuning elemeent.

1.1.2. Electro-optic birefringent external cavity laser

Faster tuning speed could be achieved by using an electro-optic(EO) birefringent filter cavity instead of a grating as the tuning element,[30-32] as shown in Fig.1.3. The EO filter is usually a $LiNbO_3$:Ti single mode strip waveguide made on a $LiNbO_3$ substrate, and consists of an electrically tunable TE-TM mode converter and a polarisation filter. The centre frequency of the device can be tuned by biasing the TE-TM mode converter, therefore selecting the oscillation mode of the laser. Continuous tuning can be realised by varying the bias to the polarisation filter.[30] With this scheme, linewidth < 60kHz, discrete tuning over 7nm, with continuous tuning of more than 1GHz, and tuning speeds up to 250 MHz were achieved.[33] Due to the short response time of the EO crystal, the tuning speed can potentially be very high.[31,32] The main disadvantage of this external cavity laser is its incompatibility with semiconductor materials, therefore precluding monolithic integration, and the very large (>100 V) drive voltage needed for wide tuning range.

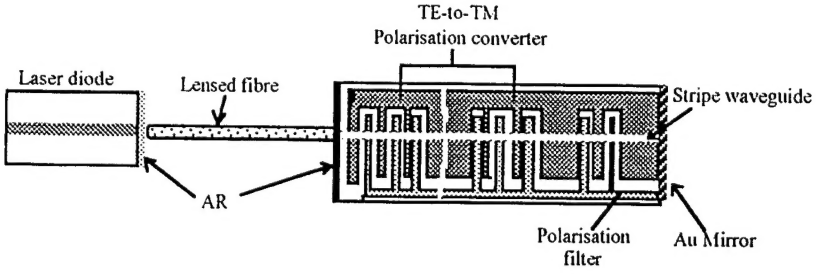

Fig. 1. 3 Electro-optic tunable laser.

1.1.3. Acousto-optic (AO) external cavity laser

Another alternative method for achieving fast tuning in external cavity laser uses acousto-optic (AO) filters.[34-36] The basic configuration is shown as Fig.1.4. A radio frequency (RF) signal is applied to the AO filter. The applied RF signal in the crystal causes an acoustic wave to be set up within it, forming a phase grating.[35] The period of the phase grating can be changed by changing the frequency of RF signal applied to the AO filter. This phase grating selects the oscillation mode in the cavity. The centre frequency of the device can be changed by simply changing the signal frequency to the AO filter. If several RF signals with different frequencies are applied to the filter at

the same time, multiple gratings can be created in the filter, allowing simultaneous lasing at several discrete wavelengthes.[34,36] In this system, centre wavelength may be shifted due to the modulation on AO filter.[36] To overcome this drawback, two AO filters with the same driving frequency can be used in the cavity, to achieve stable mode oscillation. Discrete tuning of 83 nm by varying the driving frequency between 69.4 and 74.6 MHz for a 1.3 μm laser, with a switching time of 3 ms,[36] and 35 nm tuning range for a 0.85 μm laser with switching time of 10 ns have been reported.[37]

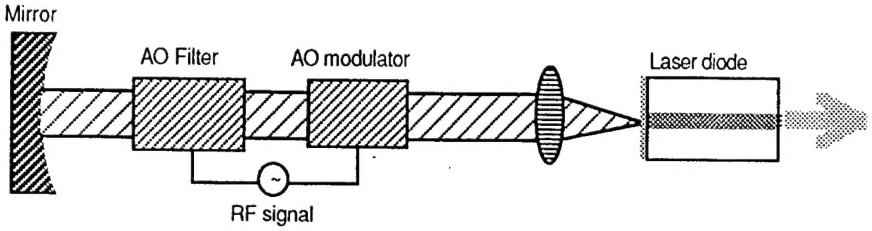

Fig. 1. 4 Acoustic-optic external cavity laser.

The main disadvantage is that the configuration is incapable of achieving continuous tuning. Also, it is difficult to achieve single mode operation, and the tuning speed is intrinsically limited by the AO elements.

In conclusion, the advantages of external cavity tunable lasers are the very wide discontinuous tuning range, almost as wide as the gain bandwidth, and the very narrow linewidth. The disadvantages are the mechanical instability and the necessity for very precise optical alignment. AR coating with very low residual reflectivity on one facet of the semiconductor is generally required for stable continuous tuning operation. Wide range continuous tuning is very difficult. High speed tuning (> 1GHz) may be possible for the EO external cavity scheme. The cavity round-trip frequency of the laser light, typically from hundreds of MHz to several GHz, defines the ultimate limit of the switching time.

1.2. Monolithic semiconductor tunable laser

Monolithic tunable lasers generally consist of two or more sections made on a single semiconductor substrate. Since they requires no external cavity, they are much smaller than the external devices. In addition to their small size, they have many other advantages, such as their mechanical stability, fast switching time, suitability for industrialised product environment and removed requirement for optical alignment.

For all types of monolithic tunable lasers, the wavelength tuning is achieved by changing the refractive index in the gain (active) or/and modulation (passive) section. One of the simplest ways to do this is to utilise the refractive index thermal effect of the semiconductor materials, by changing the temperature in the cavity to tune the emitting wavelength of the laser.[38] Since the thermal relaxation time is a slow process, the tuning speed is limited to a few MHz. Since the

tunability, tuning speed and output power stability of monolithic lasers based on thermal tuning mechanisms are much poorer than for other tuning mechanisms, we will put our emphasis on other monolithic tunable lasers.

The very successful and well developed method of achieving refractive index change is by changing the injection currents into the gain or/and the modulation section. Due to the free-carrier absorption (named the plasma effect) and the carrier induced absorption edge shift (named the band filling effect), the change in injection current changes the refractive index of the cavity.[40] Since injected carrier relaxation and recombination are faster processes than thermal changes, the tuning speed of this method is generally limited by the recombination process in material pumped below transparency.

Some types of carrier injection tuned lasers can give a nominally flat frequency modulation (FM) response within a certain frequency range[41], that is the FM modulation response is nearly a constant until the cut-off frequency which is usually determined by the injection carrier lifetime. Due to the thermal effect caused by current injection at low frequency (<1MHz), and the photon-carrier interaction and carrier modulation effects, the FM modulation response can only be maintained uniform over a limited frequency range.[39]

Monolithic tunable lasers can be classified into four types: (1) multi-segment Fabry-Perot structures; (2) Distributed Bragg reflector (DBR) structures; (3) Distributed feedback (DFB) structures and (4) Twin-guide (TG) structures. In the followed sections, we will review the progress in these areas.

1.2.1. Monolithic tunable lasers based on multi-segment Fabry-Perot structure

The earliest developed monolithic tunable laser was based on two segment Fabry-Perot (FP) structure,[42] as shown in Fig.1.5(a). It consisted of two electrically isolated sections; the modulator section and gain section. The gain section had a tapered active layer. The two sections shared a single waveguide layer. The tuning principle is simple: when a semiconductor material is placed in an electric field, due to the mixture of the linear electro-optic (LEO) effect[43] and the Franz-Keldysh (FK) effect[44] in the bulk semiconductor, the refractive index will change with the applied field. In order to have large electric field range, the modulation section was designed to be reverse biased. Both of the effects only introduce very small changes in refractive index (less than 0.3%),[43,45,46] so that the tuning range is rather limited. However, because of the nature of the field induced effect, the tuning speed, which is not limited by any carrier life time or thermal equilibrium, could be very fast.[46] Obviously, the optical length change introduced by the refractive index change will produce continuous tuning. A 15GHz continuous tuning range was obtained with this device.

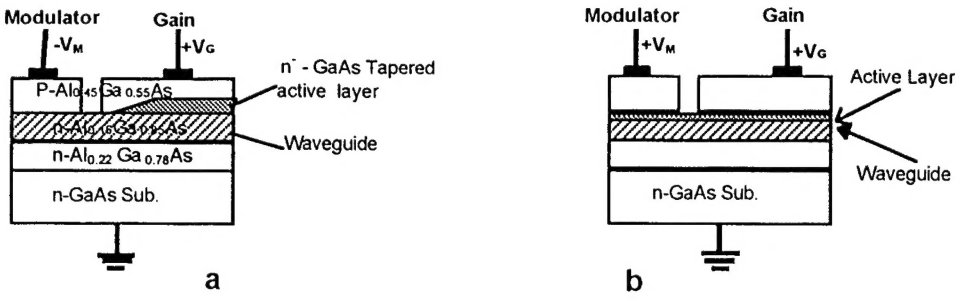

Fig. 1.5 Two-segment Fabry-Perot tunable lasers.

Another two segment, single cavity Fabry-Perot tunable laser, which was similar in structure, but quite different in tuning principle, was proposed,[47,48] as shown in Fig.1.5(b). The difference was that the modulator section was forward biased so that tuning was achieved by carrier-induced refractive index change.[40,49,50] This effect produced less than 1% refractive index change (proportional to carrier density), but still larger than that produced by LEO or FK effects in GaAs/AlGaAs material system. Continuous tuning was achievable. Since the maximum relative change of carrier density in the tuning section was limited when the gain section was lasing and the photon field was distributed in the whole single cavity, the tuning range was small (~ 0.8 nm). However, by carefully choosing the injection current ratio, it is possible to have a constant power output over the tuning range. The tuning speed was decided by the injection carrier life-time (~ns scale), which is slower than that of the field induced effect.

An unusual design,[51] which asymmetrically inserted two different quantum wells in the active layer to broaden its gain spectrum, achieved the large quasi-continuous tuning range of 22 nm by non-homogeneous current injection into the two sections.

In order to achieve large tuning range, a different two segment FP cavity laser was developed.[52,53] As shown in Fig.1.6., it consisted of two normal FP cavity lasers mounted closely on the same heat sink. The active layers are self-aligned and very closely coupled to form a two-cavity resonator. The gap between the two cleaved facet was less than 5 μm, and it acted to separate the two sections electrically. All facets were crystallographic mirror-flat and were parallel to each other, therefore, this device was called the cleaved-coupled-cavity laser or C^3 laser. In this structure, the gain and modulator sections had separate waveguides and hence the modulator acts as a mode selection element. Tuning was achieved by changing the current injection into the modulator to change the coincident mode of the two FP cavities. It obviously was a discrete tuning scheme. A tuning range of 30 nm (1.3 μm laser) and switching time ~2ns, with linewidth 8 MHz and a claimed flat FM response up to 150 MHz was reported.[53]

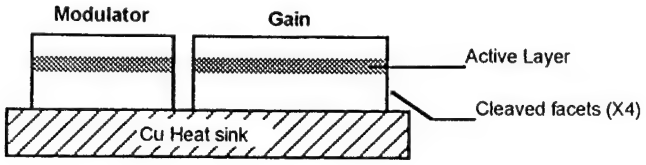

Fig. 1.6 Cleaved-coupled-cavity (C^3) laser.

In principle, by combining the above single cavity and separate cavity structures, continuous tuning over a large range should be possible. For example, a two segment single cavity as the gain and mode shift section combines with a separate mode selecting cavity.[54] However, because the optical length change will affect the coupling between the two cavities, the trade-off has to be made between wavelength stability, power output stability and tuning range. The co-ordination needed between mode shifting and mode selecting to achieve smooth continuous tuning over large range is also very difficult. Quasi-continuous tuning over a large range is more realistic.

1.2.2. DBR based monolithic tunable lasers

The most successful monolithic tunable lasers are based on DBR or DFB structures,[56] and enormous effort has been devoted to these over the past decade.[57-101] The tuning principle behind DBR or DFB lasers is simple.[65] The operating wavelength of such a laser is determined by the Bragg wavelength l_o which is related to the etched Bragg period L by $l_o = 2n_e L/m$, where n_e is the effect mode index and m the diffraction order of the Bragg grating.[55] Even though the grating period L is fixed during device fabrication, the lasing wavelength could be changed by changing the mode index n_e , which can be done by varying the injection current into the grating region. In general, n_e decreases with increasing carrier density, resulting in a shift of Bragg wavelength and hence the lasing wavelength shifts toward shorter wavelengths.

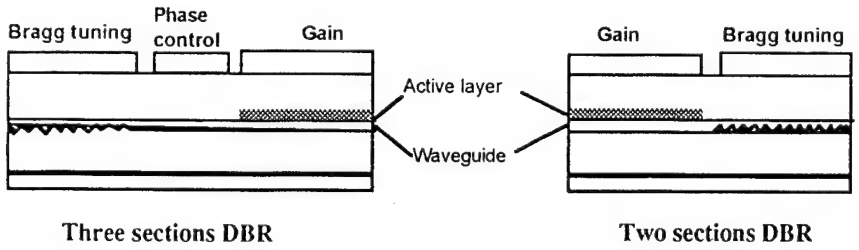

Fig. 1.7 Multi-section tunable DBR laser.

There are many schemes used to design tunable DBR lasers.[57-74] The three section tunable DBR laser[57-66] shown in Fig.1.7 has the widest continuous tuning range of any monolithic tunable laser. It consists of three sections refered to as the active (gain) section, the phase-control section and the Bragg tuning section. The three sections are optically coupled through a single waveguide, but electrically isolated from one another to allow independent current injection. The Bragg section serves as a mode selecting element which changes the Bragg wavelength of the cavity discretely

though carrier-induced refractive index change, and the phase-control section serve as the mode shift element to change the mode phase continuously.[65] The maximum discrete tuning range is determined by the maximum change in the refractive index of the Bragg section, which is less than 1%. The tuning limit also results from the limited available variation range of the carrier density owing to light-generated carriers. Since the refractive index increases with temperature,[67,68] the temperature increasing effect that accompanies the increase in tuning current partly cancels the effective refractive index decrease caused by the injected current increase. Another factor limiting the tuning range is the output power reduction resulting from the increase in free-carrier absorption loss that accompanies an increase in the tuning current. This is the reason that the tuning range is smaller at higher output power.

With this three-section DBR structure, continuous tuning over more than 6 nm was achieved,[69] 10 nm quasi-continuous tuning at 5 mw output has also been reported[57] in which the resonant mode was selected by changing the DBR section current and the narrow range tuning was done by changing the phase-control current in the vicinity of the mode.

It is possible to extend the tuning range by reverse biasing the Bragg section. A tuning range of 22 nm was obtained[70] by changing the current from -120 mA to 120 mA where the negative current corresponds to reverse biasing. The physical mechanism behind the reverse biasing tuning is local heating effect. Since refractive index increases with an increase in temperature, the lasing wavelength shifts toward to the red side, just in contrast with the blue shift caused by the forward biasing, therefore, extending the whole tuning range. A disadvantage of the thermal tuning is that the switching time is very slow (~ 100 μs) comparing with the forward biasing case (~ 1 ns).
Two-section DBR structures, which have no phase-control section, have also been reported.[71-73] However, the continuous tuning is restricted to within a longitudinal mode space, that is less than 1nm for 1.55 μm lasers.[72] An 11.6 nm discrete tuning range has been obtained for this structure.[73]

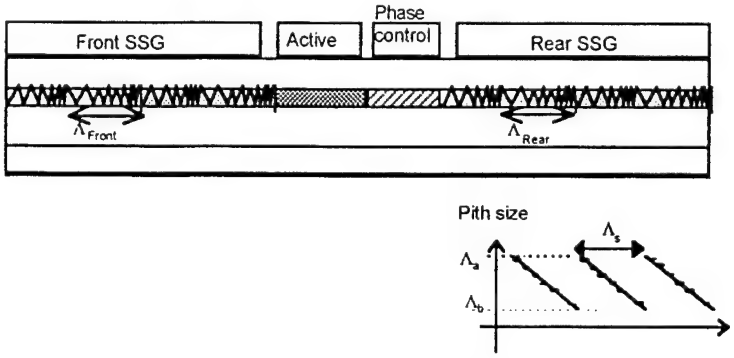

Fig. 1. 8 Schematic structure of super structure grating (SSG) DBR laser.

Recently, a new type of Bragg reflector DBR tunable laser has been proposed,[74,75] the super structure grating (SSG) DBR laser.[74] Shown in Fig.1.8 is the basic structure of this laser. It consists of an active section, front SSG-DBR section and rear SSG-DBR section,[74] a phase-control

section can be inserted between the active and the rear SSG-DBR section in some structures.[75] The SSG consist of a periodically chirped grating with a long period of L_s, and within each chirped grating, the grating pitch is linearly chirped from L_a to L_b , resulting in periodic multiple reflection peaks in the SSG reflection spectrum. Most of the reflection peaks exist in the range between l_a (= $2n_eL_a$) and l_b ($=2n_eL_b$), which could be a very wide range. The front and rear SSG-DBR are designed to have small difference in the chirped grating period L_s, allowing the laser to oscillate at the wavelength where the reflection peaks of the two reflectors coincide with each other by adjusting the injection current in the two sections. The oscillation wavelength is broadly tuned by shifting the coincident peaks even if the change of the refractive index is small. Tuning ranges as wide as 80 nm for a 1.55 μm laser, with single longitudinal mode operation and about 10 MHz linewidth, have been achieved with this structure,[74] and 105 nm tuning range with single longitudinal mode operation was obtained for multi-phase-shift SSG-DBR laser.[75] Obviously, the tuning is discrete or quasi-continuous, but is nonetheless useful for wavelength division multiplexed communication systems.

For DBR structure tunable lasers, the linewidth becomes a few times wider than when there is no tuning current injected,[59] normally 10 to several 10s of MHz. The reason is partially due to the increase in free-carrier absorption losses in the tuning sections. The frequency/wavelength switching time is basically limited by the injection carrier life time in the tuning sections. For the 1.55 μm three-section DBR laser, 200 Mbit/s frequency switching between two channels separated by 2.11nm has been carried out.[76] A claimed 'flat' FM response up to a few hundred MHz was obtained when the phase-control or the DBR section current was modulated.[72] The FM efficiency was several GHz/mA which is larger than that of a normal DFB structure laser.

1.2.3. DFB based monolithic tunable lasers

Tunable DFB lasers can be classified into two types: multi-electrode DFB lasers[63,77-81] and phase controllable DFB lasers.[82-84] In a phase-controllable DFB laser, there is no Bragg reflector in the phase control section. As shown in Fig.1.9 is a typical 2- or 3-electrode DFB laser. The tuning principle is almost the same to tunable DBR laser except that the Bragg reflector is distributed over

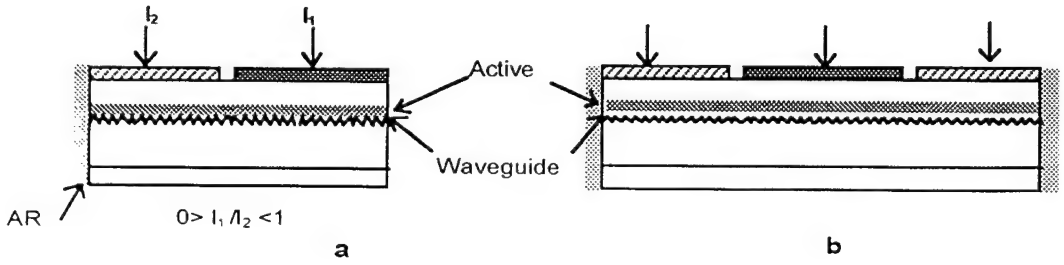

Fig. 1.9 Multi-electrode tunable DFB laser.

the whole cavity, so that a change in carrier density in one or more sections will change reflected light phase from grating pitches, the reflectivity of the grating, the gain distribution in the whole cavity and the central wavelength of the Bragg reflector, resulting in a change in threshold condition and therefore operating wavelength. Therefore, in DFB structures, the mode shifting and mode selecting function is naturally combined, and the lasing wavelength is tuned by changing the gain distribution or the threshold condition which can be done by changing the injection current ratio.[79] With an asymmetric DFB structure as shown in Fig.1.9(a), the optical field is higher in the region near the AR coated facet, resulting in a non-uniform carrier density distribution along the cavity. If the current ratio I_1/I_2 is changed, carrier density and gain distribution as well as threshold condition are changed, and the lasing wavelength is tuned.[78] An interesting configuration for a three-electrode DFB laser is with the two outer electrodes electrically connected to a common current supply whilst the central electrode was supplied with another current.[81] This device displayed a 2 nm continuous tuning and more specially, a spectral linewidth of only 500kHz. Since the carrier injection variation in the cavity influences the gain distribution and the central frequency of the filter when the lasing frequency is tuned, it is normally difficult to maintain constant optical output for this type of DFB tunable lasers[78] Fig.1.10 is a typical 2- or 3-electrode phase controllable DFB laser, that allows almost independent control of lasing wavelength and output power and is quite similar to the DBR structure case. In some newly developed designs which utilised the chirped grating DFB[85,86] or SSG structures[87] as the tuning mechanisms, continuous tuning of 5.5nm[86] and discrete tuning of 86nm[87] were achieved, which were quite similar to the results obtained by DBR structures with similar configurations.

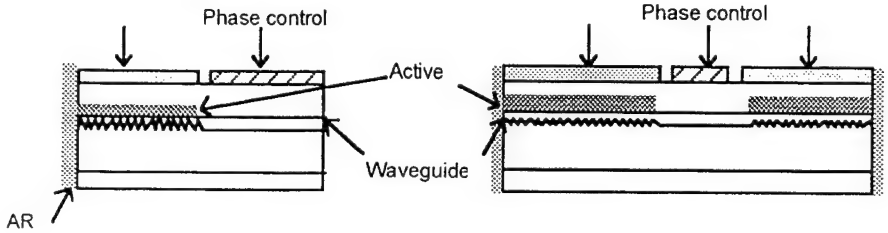

Fig. 1. 10 Phase controlable DFB tunable laser

For a 1.55 μm two-electrode DFB laser, continuous tuning ranges of 3.3 nm and 1.9 nm were achieved under 1 and 5 mW output power, respectively.[77] For a three-electrode DFB laser, normally the continuous tuning ranges were smaller than 1 nm,[79,80] but 2 nm tuning in some design was also reported.[81] For phase controllable DFB lasers, continuous tuning of 1.2 nm centred at 1.54[82] μm and 0.9 nm at 1.55 μm[83] have been reported.

Spectral linewidth of the tunable DFB laser is generally 10 MHz to 15 MHz.[77] Carefully designed structures were reported to have linewidth narrower than 4 MHz over the whole 1nm tuning range.[79] 500kHz linewidth was also reported.[81] These values are narrower than those of tunable

DBR lasers. This is probably because, for a multi-electrode DFB laser, there is no increase in absorption loss when the injection current increases.

The tuning switching time is determined by the carrier life time. A switching time of <1ns was obtained when the laser was tuned over a 1.7nm range.[88] For a multi-electrode DFB laser, the switching time would be expected to be shorter than that of a tunable DBR laser because, due to the stimulated emission in the gain cavity, the carrier life time is shorter. A claimed 'flat' FM response up to several hundred MHz has been reported for both multi-electrode[77] and phase controllable DFB laser.[82] FM efficiency of 1GHz/mA with 'flat' FM response up to 1GHz[79] and 0.67GHz/mA modulation efficiency with 'flat' FM response up to 4GHz[88] were also obtained.

1.2.4. Twin-guide tunable laser

As seen above, the tunable DBR lasers usually have low output power due to the carrier absorption loss in the long tuning sections and the DFB tunable laser is hard to tune over a wide frequency range with constant output power and linewidth. In order to achieve independent control over lasing and tuning operation, a twin-guide (TG) structure was proposed, and tunable twin-guide (TTG) lasers were realised.[89-98] In this structure, as shown in Fig.1.11, the gain and tuning are carried out in two separate layers. The two layers are electrically isolated to enable independent current and bias operation in both layers, but are optically coupled transversely to form a twin-guide cavity. The effective refractive index of the cavity can be changed by changing only the injection current in the tuning layer, without disturbing the carrier density or the gain distribution in the active layer. Therefore, the output power can be maintained constant while the lasing frequency is tuned.

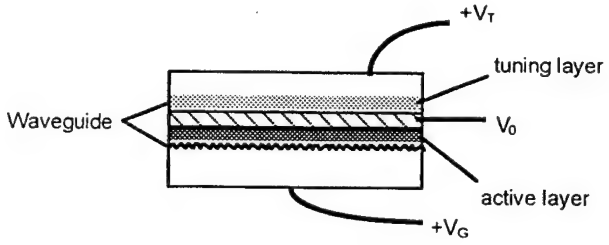

Fig. 1.11 Twin-guide tunable DFB laser.

This device exhibits a strictly continuous tuning with no mode jumps or other wavelength ambiguities.[95] Continuous tuning ranges of over 10nm at 1.55μm have been reported,[92] by both forward biasing (thermal tuning) and reverse biasing (electronic tuning) the tuning region. Over a tuning range of 9.2nm, with output power above 1mW, a spectral linewidth below 30MHz was also achieved.[92] With a coupled grating-assisted filter structure,[93] discrete tuning as wide as 57nm was also reported. Output power as high as 10mW, with continuous tuning of 1.2nm in a 1.55μm TTG laser was also obtained.[96] The spectral linewidth of this devices is normally broadened (about 10~60MHz) while tuning the frequency due to the different mechanisms,[97,99-101] but with specially designed structures, such as the complimentary twin-active-guide (CTAG) laser, the linewidth could be maintained at a constant (~ 10MHz) over a certain tuning range (~2nm).[97] A very narrow

linewidth (0.5~9MHz) TTG laser was also achieved.[101]

In conclusion, the monolithic tunable lasers developed so far are all based on the refractive index change by a certain kind of physical mechanism. Thermal, electric field or current induced effects are all demonstrated to be usable mechanisms in achieving refractive index changes, and among them, field and carrier density induced effects are the more attractive ones due to their faster response. The field induced effects, mainly LEO and FK effects, offer small refractive index change (<0.3%), but potentially fast tuning speed. A tunable laser based on field induced LEO and FK effects with FP cavity has achieved 15 GHz continuous tuning. Carrier density induced refractive index change is the most widely studied and extensively used mechanism in all different configurations of monolithic tunable lasers as it can provide nearly 1% refractive index change, which is much larger than that by field induced LEO or FK effects. According to their waveguide or cavity forms, monolithic tunable laser may be classified into FP, DBR, DFB and TG lasers. Generally, multi-segment FP has small continuous tuning range or relative large but discrete tuning, and it is easy to achieve stable power output. DBR lasers give the largest tuning range, good tunability and stable but low output power, due to the high absorption loss in relatively long tuning sections. DFB lasers give higher output power and good tuning range, but it is difficult to maintain constant power output. Its tuning performance is also more complicated. TTG lasers which provide independent control of output power and tuning and offer the best combination of tunability and power operation, is the best monolithic tunable laser developed so far. By using very complicated chirped grating or SSG structures, the tuning range can be extended further to over 100nm. The tuning speed of the tunable laser based on carrier induced effect is limited by the carrier life time which is around several ns, and the tuning range is generally limited by the available refractive index change. Due to the injection current thermal effect, the FM response of the tunable laser tuned by carrier injection is not flat at low frequencies (<1MHz), and it is also never strictly flat when modulation frequency is higher than 1MHz because of photon-carrier interaction and carrier modulation effects. For tunable lasers based on Bragg grating reflectors, the fabrication processing is quite complicated, as the fabrication of Bragg grating reflector and re-growth processes are needed.

1.3. Tuning technique based on quantum-confined Stark effect (QCSE)

So far most of the electronic tuning mechanisms are based on carrier induced refractive index change. The refractive index change due to this effect is limited and normally less than 1%.[50] For coherent systems, tunable lasers based on this effect suffer from the drawback of rigorously non-flat FM response due to thermal effects. Field induced tuning, due to its independence of thermal or carrier influence, results in much faster tuning speeds and, more importantly, provides a possible method of achieving rigorously flat FM response. Unfortunately, the possible tuning range provided by LEO or FK effects is very small. In order to have wider tuning range, larger refractive index change mechanisms are required. With the rapid development of semiconductor ultrathin layered (~100Å) structure growth technology, many new phenomena related to the dimensionally confined quantum mechanical nature of a quantum well (QW) or a multi-quantum well (MQW)

structure have been discovered.[102] Among them, the quantum-confined Stark effect (QCSE), which changes the optical properties of the QWs when electric fields are applied perpendicular to the QW layers, displays field-induced refractive index changes much larger (as large as 4%) than that due to carrier injection. This effect obviously has important applications in tunable lasers.

1.3.1. Quantum-confined Stark effect (QCSE)

Since the enormous progress in semiconductor growth technology, mainly in metal-organic chemical vapour deposition (MOCVD) and molecular beam epitaxy (MBE), the idea of growing very thin layered semiconductor structures became realistic. As the high quality QW structures can be grown successfully, much interest was attracted to study in this area.[102]

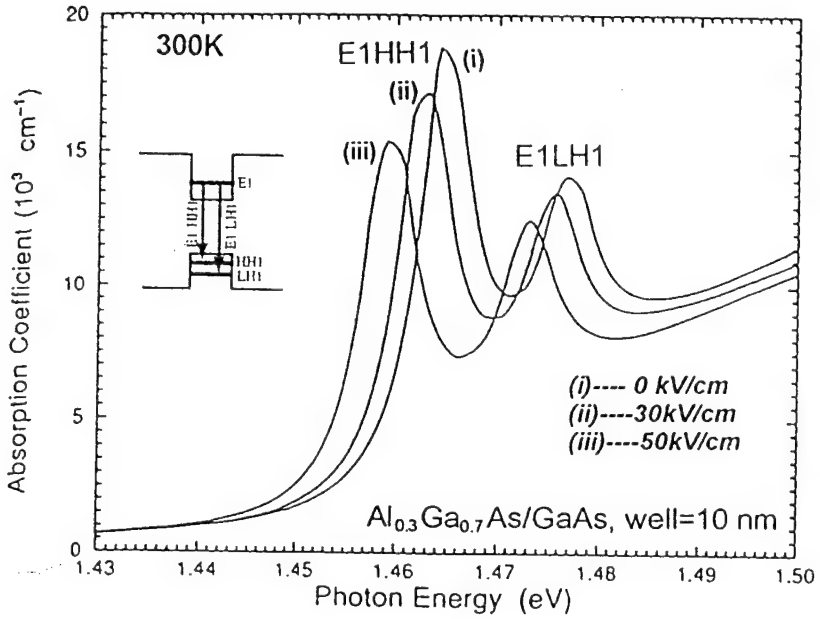

Fig.1.12 Optical absorption spectrun shows the exciton peaks variation with electric field in a QW structure material.

Normal bulk semiconductors show an absorption spectrum near their band gap energy that is relatively smooth and featureless at room temperature. QWs, such as AlGaAs/GaAs/AlGaAs, on the other hand, show a clear series of steps or peaks, as shown in Fig.1.12. These steps result from the fact that electrons and holes are confined in the GaAs quantum well by AlGaAs barriers, and then a series of bound states in the QW are produced. The steps or peaks correspond to the different transitions between the bound states in the valence band and conductive band. For each confined state of electron and hole, the lowest-energy electron-hole pair state is the exciton, in which the electron and hole orbit around one another just like a hydrogen atom. The strength of an optical transition is generally proportional to the wavefunction overlap of the electron and hole, and in the case of an exciton, this is larger because they are in a tighter orbit around each other, hence the stronger absorption peak. Excitonic effects in the QWs are particularly large because the overlap of wavefunctions between electron and hole has to be larger by being confined inside the QW. This

effect is so large that the exciton peak can be seen even at room temperature.[103] Many non-linear optical effects are associated with these exciton peaks.[103,104] The most interesting effect among them is the QCSE.[105,106] One of the most important consequences of this effect is that the sharp optical absorption edge near the band gap energy can be shifted, by a perpendicularly applied electric field, to lower energy without destroying the sharp exciton absorption peaks.[107-109] This contrasts strongly with the behaviour of bulk materials, in which the exciton peaks are all but unresolvable at room temperature, and are destroyed with moderate fields, and the remaining absorption changes correspond to a broadening of the absorption edge. This field effect in bulk materials is often referred to as the Franz-Keldysh effect.[44]

The physics of the QCSE is relatively well understood.[105,106,110] The reason for the persistence of the exciton peaks is that the barriers of the QW structure prevent the electron and hole from being separated by the field, which prevents lifetime broadening of the exciton resonance. The shift of the exciton resonance with field is simply equivalent to the Stark shift that would happen in a strongly confined hydrogen atom. This is the reason the effect was titled as QCSE. The relationship between the QCSE and the Franz-Keldysh effect is now understood.[110,111] The absorption does become somewhat weaker as the absorption edge shifts to lower energy under the field because the electron-hole overlap is reduced by the electron and hole being pulled to opposite sides of the well.

There is in fact another effect based on QW structure. When the barrier thickness is small enough that the quantum wave in one well can penetrate the thin barrier and couple with the quantum wave in a neighbouring well (resonant tunnelling), a coupled QW structure[112] results. The superlattice (SL) structure is a stack of many such coupled MQW structure[113]. The excitonic characteristics of the SL structure, in our context, is quite similar to that of a non-coupled MQW structure,[114] and its field effect which is called the Wannier-Stark effect,[115] is also similar to QCSE.

One of the important result of the QCSE is that we obtain a new and strong electroabsorption mechanism in semiconductors. The changes in absorption are so large that it is possible to make optical modulators that are only micrometres thick and whose transmission can be changed by more than a factor of 2 with voltages ~5 to 10V. Indeed, based on QCSE, some non-linear optical devices have already been demonstrated.[116-120] Because of QCSE, large field-induced refractive index changes are possible,[121-124] which provide new possibilities for monolithic tunable lasers.

Theoretically, the switching time of the field-induced effect is limited only by the lattice thermalisation and relaxation time of the structural materials, which is normally less than 10ps.[125] Therefore, a tunable laser based on QCSE should have much higher tuning speed than that based on carrier life-time limited effects together with a flat FM response.

1.3.2. Tunable laser based on QCSE

A few tunable lasers based on QCSE have been demonstrated.[15,16,126] Both external cavity[15,16] and integrated monolithic twin-guide DFB laser[126] schemes were adopted.

The external cavity tunable laser using QCSE demonstrated by our group is the earliest experiment to use QCSE in tunable lasers.[15] Fig.1.13. is the schematic diagram of this device. The tuning element is a normal incident MQW p-i-n diode grown by MOVPE (metal-organic vapour phase epitaxy), which allows large reverse bias to be applied across the intrinsic i-MQW layers so

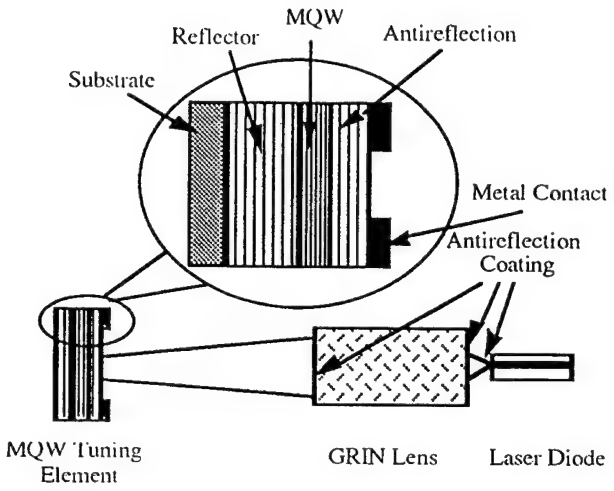

Fig. 1.12 External cavity tunable laser by using QCSE.

achieving a large variation of electric field. By varying the reverse bias in this tuning element, the refractive index in the tuning region is changed due to the QCSE, therefore continuous tuning (with AR coated laser) or discrete tuning (with no AR coated laser) is achievable. By using this set-up, discrete tuning of 600 GHz with a reverse bias change of 6V15 and continuous tuning of more than 2GHz for a reverse bias change of 5V16 were obtained. In the continuous tuning experiment, more than 2GHz tuning range corresponding to a refractive index change of about 3% was confirmed.16 Good linearity between tuned frequency shift and the reverse bias and less than 0.3dB output power change were observed over a tuning range of 1.5GHz.16 A uniform FM response within 3dB from 20kHz up to 1.2GHz was obtained. The response cut-off at high frequency was not caused by QCSE mechanism itself, but by the parasitic parameters of the device. By reducing these parasitics a tuning element response extending to 20GHz and flat FM response for this system up to 6GHz were predicted.16 A response limit in excess of 50GHz for an integrated monolithic tunable laser using QCSE was also predicted.

T. Wolf *et al* have demonstrated a tunable twin-guide laser using QCSE.[126] The structure of the monolithic TTG laser is shown in Fig.1.14.

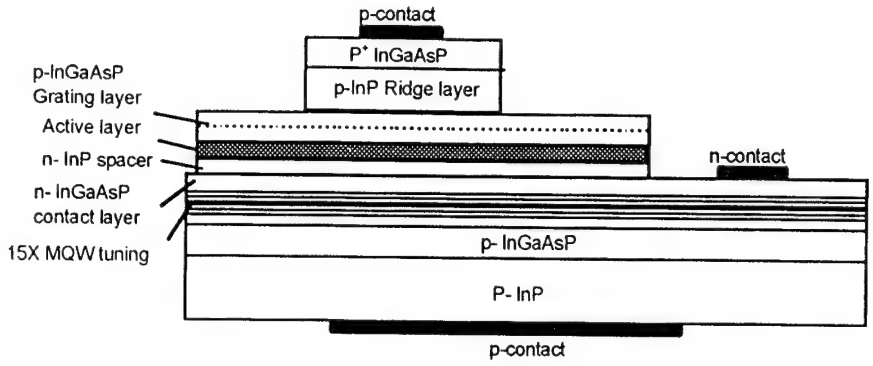

Fig. 1.14 Schematical cross section of QCSE-TTG laser with ridge waveguide structure.

The device is grown by a two step MOVPE process. After the first MOVPE growth the DFB grating on the top layer was etched and then a second MOVPE overgrowth process was performed. In order to achieve best tunability, careful design was adapted to make the gain region emit at wavelength 1555nm and the MQW tuning region have a photoluminescence peak at 1380nm to enable a ~100meV energy difference between the photon energy and the absorption edge in the MQW layer. For a 600μm long device, when a 3V reverse bias was applied to the tuning layer, optical output power dropped from 5 mW to 3 mW, correspondingly, threshold current increased from 94mA to 104mA. For an 800μm cavity device, the best output power of 10mW and linewidth 3.7MHz were achieved. It was found that the absorption in the MQW structure increases with electric field, and this effect corresponded to the increase in threshold current at higher field. A tuning range of about 15 GHz with reverse bias variation from 0~3V has been demonstrated. At lower bias (<1.5V), the frequency shift is dominated by the refractive index change with bias, but at higher bias, due to the increased absorption, the frequency shift with bias tends to be saturated. A flat FM response with 7GHz/V efficiency up to 2GHz and with a 3dB modulation bandwidth of 1GHz was obtained. The advantage of this device is its independent controllability of gain and tuning regions, in both electrical control and structure optimisation. The disadvantage is also obvious: in addition to the requirement for re-growth processing and the complicated fabrication, the separating layer needed at the middle of the waveguide reduces the optical field coupling, thus reduces the tuning sensitivity.

Based on the Wannier-Stark effect of SL structure, J. Langanay *et al* realised a tunable laser based on a DBR structure[127]. In the device, the active region is five QWs of 8 nm-thick InGaAsP 1% strained separated by a 10 nm-thick InGaAsP unstrained barrier, and the tuning region, i.e. the phase control and Bragg sections consists of 15 6.6 nm thick InGaAs quantum wells separated by 2.6 nm InP barriers. The two regions are butt-jointed by three steps gas source MBE growth. The FM and AM -3dB cut-off frequency is 350MHz when the device is forward biased, while it reaches 4GHz when it is reverse biased to 2.6 V. The FM response efficiency is 3.1± 0.7 Å/V, and the response is not flat due to non-optimised design.

In conclusion, QCSE proved to be able to provided larger refractive index changes than those due

to carrier induced effects, and more importantly, the potential tuning speed using field induced QCSE is much faster, with the advantage of providing rigorously flat FM response, therefore it provides a more advanced mechanism for tunable laser control. Two pioneering experiments using QCSE as the tuning mechanism, based on external cavity configurations and TTG structure respectively, demonstrated the potential of the approach. Much further work is needed to realise a practical laser with flat FM response.

1.4 Conclusion

In this chapter, we have reviewed the tuning methods and tunable laser devices developed so far in both external cavity and monolithically integrated tunable laser systems. In the external cavity configurations, external grating cavity lasers provided the widest tuning range (160nm), but the lowest tuning speed. High speed tuning (>1GHz) may be possible for the EO external tuning scheme, but its continuous tuning range was very limited and large tuning voltages are required. In general, external cavity tuning schemes are not suitable for use in a practical system as they are too sensitive to mechanical vibration and normally require precise adjustment.

The monolithic tunable laser configurations, are based on four basic types of cavity forms, referred to as FP, DBR, DFB and TG cavities. Except for one reported two segment FP cavity tunable laser in which the field induced LEO and FK effects were used as the tuning mechanism,[42] all the other tuning configurations used the carrier induced refractive index changes as the tuning mechanism with less than 1% available refractive index change. This mechanism limited the possible tuning range and its switching speed was limited by the carrier recombination process or carrier life time. It is also unable to provide rigorously flat FM response. Monolithic tunable lasers based on Bragg grating reflectors all required re-growth processing and quite complicated fabrication processing which certainly results in high cost and low productivity.

The field induced QCSE in MQW semiconductor structures was found to have the possibility of providing as much as 4% refractive index change. Due to the fast nature of the field-induced effect, the potential tuning speed is very high (~50GHz). It also has the advantage of providing rigorously flat FM response. Two reported tunable lasers using QCSE as the tuning mechanism were based on external cavity [15,16] and TTG structures[126] respectively, and one reported DBR tunable laser based on butt-joint configuration using SL Wannier-Stark effect as the tuning mechanism,[127] achieved promising results and displayed very good prospects for future development.

1.5 References

1. H. Toba, K. Oda, K. Nakanishi, N. Shibata, K. Nosu, N. Takato and M. Fukuda, J. Lightwave Tech., LT-8, 1396(1990).
2. T. Li, "Advances in optical fibre communications: an historical perspective", IEEE J. Select. Areas Commun., SAC-1, 356-72(1983).

3. T. L. Koch and U. Koren, "Semiconductor laser for coherent optical fibre communications", *J. Lightwave Tech.*, **LT-8**, 274-93(1990).
4. Y. Suematsu, S. Arai and F. Koyama, "Dynamic singal mode lasers", *Optica Acta*, **32**, 1157-73(1985).
5. G. P. Agrawal and N. K. Dutta, *Semiconductor Lasers*, 2nd Edition, p18(1993).
6. T. Okoshi and K. Kikuchi, *Coherent Optical Fibre Communications*, Boston: Kluwer Acadmic, 1988.
7. G. P. Agrawal, Chap.6, in *Fibre-Optic Communication Systems*. New York: Wiley Interscience, 1992.
8. R. A. Linke and A. H. Gnauck, "High -capacity coherent lightwave systems", *J. Lightwave Tech.*, **LT-6**, 1750-69(1988).
9. T. G. Hodgkinson, R. Wyatt and D. W. Smith, "Experimental assessment of a 40 Mbit/s coherent optical receiver at 1.52 μm", *Electron. Lett.*, **18**, 523(1982);

   F. E. Goodwin, "A 3.39 μm infrared optical heterodyne communication system", *IEEE J. Quantum Electron.*, **QE-3**, 524-31(1967).
10. T. Okoshi, "Recent advances in coherent optical fibre communication systems", *J. Lightwave Tech.*, **LT-5**, 44-51(1987).
11. D. W. Smith, "Techniques for multigigabit coherent optical transmission", *J. Lightwave Tech.*, **LT-5**, 1466-78(1987).
12. L. G. Kazovsky and G. Jacobsen, "Multichannel CPFSK coherent optical communication system", *J. Lightwave Tech.*, **LT-7**, 972-82(1989).
13. T. Chikama, T. Naitou, H. Onaka, T. Kiyonaga, S. Watanabe, M. Suyama, M. Seino and H. Kuwahara, "1.2 Gbit/s, 201 km optical DPSK heterodyne transmission experiment using a compact, stable external fibre DFB laser module", *Electron. Lett.*, **24**, 637-7(1988).
14. Y. Imai, K. Iizuka and R. T. B. James, "Phase-noise-free coherent optical fibre communication systems utilizing differencial polarisation shift keying(DPolSK)", *J. Lightwave Tech.*, **LT-8**, 691-8(1990).
15. B. Cai, A. J. Seeds, A. Rivers and J. S. Roberts, "Multiple quantum well-tuned GaAs/AlGaAs laser", *Electron. Lett.*, **25**(2), 145-6(1989).
16. B. Cai, A. J. Seeds and J. S. Roberts, "MQW tuned semiconductor lasers with uniform frequency response", *IEEE Photon. Technol. Lett.*, **6**(4), 496-8(1994).
17. K. Y. Liou, C. A. Burrus, R. A. Linke, I. P. Kaminow, S. W. Granlund, C. B. Swan and P. Besomi, "Single longitudinal mode stabilised graded-index-rod external coupled-cavity laser", *Appl. Phys. Lett.*, **45**, 279(1984).
18. T. P. Lee and C. Zah, "Wavelength tunable and single frequency semiconductor lasers for photonic communications networks", *IEEE Commun. Mag.*, p45-51, October 1989.
19. C. H. Henry, 'Theory of the linewidth of semiconductor lasers', *IEEE J. Quantum Electron.*, **QE-18**(2), 259-64(1982).
20. H. D. Edmonds and A. W. Smith, "Second harmonic generation with the GaAs laser", *IEEE J. Quantum Electron.* **QE-6**, 356-8(1970).
21. P.L.Thomas, "Single longituinal mode operation of CW junction lasers by frequency selective optical feedback", *Appl. Phys. Lett.*, **25**, 744(1974).

22. F.Favre, D.Le Guen, J.C.Simon and B.Landousies, "External cavity semiconductor laser with 15nm continuous tuning range", *Electron. Lett.*, **22**, 795-6(1986).
23. K.Kobayashi, R.Ishikawa, K. Minemura and S.Sugimoto, "Micro-optical devices for fibre-optic communications", *Fibre and Integrated optics*, **2**, 1-17(1979).
24. W.J.Tomlinson, "Application of GRIN rod lenses in optical communication systems", *Appl. Opt.*, **19**, 1127-38(1980).
25. J.Wittmann and G.Gaukel, "Marrow-linewidth laser with a prism grating: GRIN rod lens combination serving an external cavity", *Electron. Lett.*, **23**, 524-5(1987).
26. D. Mehuys, M. Mittelstein, A. Yariv, R. Sarfaty and J. E.Ungar, "Optimised Fabry-Perot AlGaAs quantum well lasers tunable over 105nm", *Electron. Lett.*, **25**(2), 143-5(1989).
27. C. P. Seltzer, M. Bagley, D. J. Elton, S. Perrin and D. M. Cooper, "160nm continuous tuning of an MQW laser in an external cavity across the entire 1.3 mm communication window", *Electron. Lett.*, **27**, 95-6(1991).
28. K. Kobayashi and I. Mito, "Single frequency and tunable laser diodes", *J. Lightwave Technol.*, **6**(11), 1623-33(1988).
29. R. Wyatt and W. J. Devlin, "10-kHz linewidth 1.5 μm InGaAsP external cavity laser with 55nm tuning range", *Electron. Lett.*, **19**, 110-2(1983).
30. C. L. Tang, V. G. Kreismanis and J. M. Ballantyne, "Wide-band electro-optical tuning of semiconductor lasers", *Appl. Phys. Lett.*, **30**, 113-6(1977).
31. A. Olsson and C. L. Tang, "Electrooptically tuned external cavity CW semiconductor laser and FM optical communications", *IEEE J. Quantum Electron.* **QE-15**, 1085(1979).
32 A. Schremer and C. L. Tang, "Single frequency tunable external cavity semiconductor laser using an electro-optic birefridgent modulator", *Appl. Phys. Lett.*, **55**, 19(1989).
33. F. Heismann, R. C. Alferness, L. L. Buhl, G. Eisenstein, S. K. Korrotky, J. J. Veselka, L. W. Stulz and C. A. Burrus, "Narrow linewidth, electroptically tunable InGaAsP-Ti:$LiNbO_3$ extended cavity laser", *Appl. Phys. Lett.*, **51**, 164-6(1987).
34. T. Hidaka and T. Nakamoto, "Electric tuning of semiconductor laser using acousto-optic device", *Electron. Lett.*, **25**, 1320-1(1989).
35. S. E. Harris and R. W. Wallace, "Acoustoptic tunable filter", *J. Opt. Soc. Am.*, **59**, 744-7(1969).
36. G. Coquin, K. W. Cheung and M. M. Choy, "Single and multiple wavelength operation of acousto-optically tuned semiconductor lasers at 1.3 μm", *IEEE J. Quantum Electron.* **QE-25**, 1575-79(1989).
37. G. Coquin and K. W. Cheung, "An electronically tunable external cavity semiconductor laser", *Electron. Lett.*, **24**, 599-600(1988).
38. N. K. Dutta, T. Wessel, T. Cella and R. L. Brown, "Continuously tunable distributed feedback laser diode", *Appl. Phys. Lett.*, **47**, 981-3(1985).
S. Hava, R. G. Hunsperger and H. B. Siqueira, "Monolithically Peltier-cooled laser diodes", *J. Lightwave Technol.*, **LT-2**, 175-80(1984).
39. D. W. Smith, "Techniques for multi-gigabit coherent optical transmission", *J. Lightwave Technol.*, **LT-5**(10), 1466-78(1987).
40. J. Manning, R. Olshansky and C. B. Su, "The carrier induced index change in AlGaAs and 1.3μm InGaAsP diode lasers", *IEEE J. Quantum Electron.* **QE-19**, 1525-30(1983).

41. S. Kobayashi, Y. Yamamoto, M. Ito and T. Kimura, *IEEE J. Quantum Electron.* **QE-18**, 582(1982).
42. F. K. Reinhart and R. A. Logan, "Integrated electro-optic intracavity frequency modulation of double-heterostructure injection laser", *Appl. Phys. Lett.*, **27**(10), 532-4(1975).
43. F.K. Reinhart and B.I. Miller, *Appl. Phys. Lett.*, **20**, 36(1972)
44. W. Franz, *Z. Naturforsch.*, **13a**, 484(1958).
L. Keldysh, "The effect of a strong electric field on the optical properties of insulating crystals", *Sov. Phys. -JEPT* **7**, 788-90(1958).
45. T. E. Van Eck, L. M. Walpita, W. S. C. Chang and H. H. Wieder, "Franz-Keldysh electrorefraction and electroabsorption in bulk InP and GaAs", *Appl. Phys. Lett.*, **48**, 451-3(1986).
46. A. Alping and L. A. Coldren, "Electrorefraction in GaAs and InGaAsP and its application to phase modulators", *J. Appl. Phys.*, **61**, 2430-3(1987).
47. R. F. O'Dowd and M. G. Davis, "Theoretical study of a two-section single cavity semiconductor laser for use as a wavelength tunable source", *Opt. & Quantum Electron.*, **20**, 383-93(1988).
48 S. W. Corzine and L. A. Coldren, *Appl. Phys. Lett.*, **48**, 1190(1986).
49. C. H. Henry, R. A. Logan and K. A. Bertness, "Spectral dependence of the change in refractive index due to carrier injection in GaAs lasers", *J. Appl. Phys.*, **52**, 4457-61(1981).
50. J. G. Mendoza-Alvarez, F. D. Nunes and N. B. Patel, "Refractive index dependence on free carriers for GaAs", *J. Appl. Phys.*, **51**, 4365-7(1980).
51. S. Ikeda, A. Shimizu, Y. Sekiguchi and M. Hasegawa, "Wide-range wavelength tuning of an asymmetric dual quantum well laser with inhomogeneous current injection", *Appl. Phys. Lett.*, **55**, 2057-9(1989).
52. W. T. Tsang, N. A. Olsson and A. Logan, "High-speed direct single frequency modulation with large tuning rate and frequency excursion in cleaved-coupled-cavity semiconductor lasers", *Appl. Phys. Lett.*, **42**, 650-2(1983).
53. W. T. Tsang, Semiconductor and Semimetal, **22**, Part B, 257(1986)
54. L. A. Coldren and S. W. Corzine, *IEEE J. Quantum Electron.* **QE-23**, 903(1987).
55. D. Marcuse, *Light Transmission Optics*. New York: Van Nostrand Reinhold, Chap.2, 1982.
56. Y. Kotaki and H. Ishikawa, "Wavelength tunable DFB and DBR lasers for cherence optical fibre communications", *IEE Proc. J*, **138**, 171-7(1991)
57. S. Murata, I. Mito and K. Kobayashi, *Electron. Lett.*, **23**, 403(1987).
58. S. Murata, I. Mito and K. Kobayashi, *Electron. Lett.*, **24**, 12(1988).
59. S. Murata, S. Takano, I. Mito and K. Kobayashi, *Proceedings: International Conference on Semiconductor Lasers*, Boston, 29 Aug.-1 Sept., p122(1988).
60. Y. Kotaki, M. Matsuda, H. Ishikawa and H. Imai, *Electron. Lett.*, **24**, 503(1988).
61. M. Yamaguchi, M. Kitamura, S. Murata, I. Mito and K. Kobayashi, *Electron. Lett.*, **21**, 63(1985).
62. L. D. Westbrook, A. W. Nelson, P. J. Fiddyment and V. J. Collins, *Electron. Lett.*, **21**, 957(1985).

63. Y. Yoshikuni, K. Oe, G. Motosugi and T. Matsuoka, *Electron. Lett.*, **22**, 1153(1986).
64. K. Kotaki, M. Matsuda, M. Yano, H. Ishikawa and H. Imai, *Electron. Lett.*, **23**, 325(1987).
65. K. Kobayashi and I. Mito, *J. Lightwave Technol.* **LT-6**, 1623(1988).
66. T. L. Koch, U. Koren and B. J. Miller, *Appl. Phys. Lett.*, **53**, 1036(1988).
67. D. T. F. Marple, "Refractive index of GaAs", *J. Appl. Phys.*, **35**(4), 1241-2(1964).
68. S. Akiba, K. Utaka, K. Sakai and Y. Matsushima, *Jpn. J. Appl. Phys., Part 1,* **23**, 1054(1984).
S. Akiba, K. Utaka, K. Sakai and Y. Matsushima, *Jpn. J. Appl. Phys., Part 1,* **21**, 1736(1982).
69. T. L. Koch and U. Koren, *J. Lightwave Technol.* **LT-8**, 274(1990).
70. M. Oberg, S. Nilsson, T. Klinga and P. Pjala, *IEEE Photon. Technol. Lett.*, **3**, 299(1991).
71. Y. Thomori, H. Oohhashi, T. Kato, S. Arai, K. Komori and Y. Suematsu, *Electron. Lett.*, **22**, 138(1986).
72. S. Murata, I. Mito and K. Kobayashi, *IEEE J. Quantum Electron.* **QE-23**, 835(1987).
73. B. Broberg and S. Nilsson, *Appl. Phys. Lett.*, **52**, 1285(1988).
74. Y. Tohmori, Y. Yoshikuni, T. Tamamura, M. Yamamoto, Y. Kondo and H. Ishii, "Ultrawide wavelength tuning with single longitudinal mode by super structure grating (SSG) DBR lasers", in *Tech. Dig. 13th IEEE Semiconductor Laser Conf.*, Takamatsu, Japan, Sept. 1992, p268-9
75. H. Ishii, Y. Tohmori, Y. Yoshikuni, T. Tamamura and Y. Kondo, "Multi-phase shift super structure grating (SSG) DBR lasers for broad wavelength tuning", *IEEE Photon. Technol. Lett.*, **5**(6), 613-5(1993).
76. H. Kobrinski, M. P. Vecchi, T. E. Chapuran and J. B. Georges, *Tech. Dig. Opt. Fibre Comm. Conf., Houston*, 6-9 Feb. 1989, PD3-1.
77. M. Okai, S. Sakano and N. Chinone, "Wide range continuous tunable double sectioned distributed feedback lasers", *15th European Conf. on Opt. Commun.* (Sweden), p122-5, Sept., 1989.
78. M. Kuzetrov, "Theory of wavelength tuning in two-segment distributed feedback lasers", *IEEE J. Quantum Electron.* **QE-24**, 1837-44(1988).
79. M. Fukuta, K. Sato, Y. Kondo and M. Nakao, "Continuously tunable thin active layer and multisection DFB laser with narrow linewidth and high power", *J. Lightwave Technol.* **LT-7**, 1504(1989).
80. Y. Yoshikuni and G. Motosugi, *J. Lightwave Technol.* **LT-5**, 516(1987).
81. H. Imai, "Tuning results of 3-sectioned DFB lasers", *Semiconductor Laser Workshop, Conf. on Lasers and Electrooptics, CLEO'89*, USA, 1989.
82. S. Murata, I. Mito and K. Kobayashi, *Electron. Lett.*, **23**, 12(1987).
83. T. Numai, S. Murata and I. Mito, *Electron. Lett.*, **24**, 1526(1988).
84. H. Olesen, X. Pan and B. Tromborg, "Theoretical analysis of tuning properties for a phase tunable DFB laser" *IEEE J. Quantum Electron.* **QE-24**, 2367-75(1988).
85. N. Chen, Y. Nakano and K. Tada, "Fabrication of multiple-electrode chirped grating tunable distributed feedback lasers", *Jpn. J. Appl. Phys., Part 1,* **33**(1B), 856-8(1994).
86. H. Hillmer, H. L. Zhu, A. Grabmaier, S. Hansmann, H. Burkhard and K. Magari, "Novel

tunable semiconductor lasers using continuously chirped distributed-feedback gratings with ultrahigh spatial precision", *Appl. Phys. Lett.*, **65**(17), 2130-2(1994).

87. Y. Tohmori, F. Kano, H. Ishii, Y. Yoshikuni and Y. Kondo, "Wide tuning with narrow-linewidth in DFB lasers with superstructure grating (SSG)", *Electron. Lett.*, **29**(15), 1350-2(1993).
88. M. Horita, M. Tsurusawa, K. Utaka and Y. Matsushima, "Wavelength tunable InGaAsP-InP multiple-λ/4 shifted distributed feedback laser", *IEEE J. Quantum Electron.* **QE-29**(6), 1810-16(1993).
89. M. C. Amman, S. Ilek, C. Schanen and W. Thulke, "Tunable twin-guide laser: a novel laser diode with improved tuning performance", *Appl. Phys. Lett.*, **54**, 2532-3(1989).
90. M. C. Amman and W. Thulke, "Continuously tunable laser diodes: longitudinal versus transverse tuning scheme", *IEEE J. Sel. Areas Comms.*, **SAC-8**, 1169-77(1990).
91. S. Ilek, W. Thulke, C. Schanen, H. Lang and M. C. Amman, "Over 7nm (875GHz) continuous wavelength tuning by tunable twin guide (TTG) laser diode", *Electron. Lett.*, **26**, 46-7(1990).
92. T. Wolf, S. Illek, J. Rieger, B. Borchert and M. C. Amann, "Tunable twin-guide (TTG) disributed feedback (DFB) laser with over 10 nm continuous tuning range", *Electron. Lett.*, **29**(24), 2124-5(1993).
93. M. C. Amann and S. Illek, "Tunable laser diodes utilizing transverse tuning scheme", *J. Lightwave Technol.* **LT-11**(7), 1168(1993).
94. W. Thulke, V. Achatz, B. Borchert, S. Illek and T. Wolf, "Integratable tunable twin-guide laser on semiinsulating substrate", *Jpn. J. Appl. Phys., Part 2*, **32**(7A), L914-6(1993).
95. M. C. Amann, "Broad-band wavelength tunable twin-guide lasers", *Optoelectronics: Devices& Technol.*, **10**(1), 27-38(1995).
96. T. Wolf, H. Westermeier and M. C. Amann, "Tunable twin-guide (TTG) laser-diodes with metal-clad ridge-wave-guide (MCRW) structure for coherent optical communications", *European Trans. on Telecom. & Related Technol.*.**3**(5), 517-22(1992).
97. E. Yamamoto, M. Hamada, K. Suda, S. Nogiwa and T. Oki, "Wavelength tuning characteristics of DFB lasers having twin-guide structures modulated by injection current or electric field", *IEE Proc. J*, **139**(1), 24-28(1992).
98. E. Yamamoto, M. Hamada, K. Suda, S. Nogiwa and T. Oki,"Wavelength tuning characteristics of tunable twin-guide lasers with improved current-injection structures", *Appl. Phys. Lett.*, **60**(7), 805-6(1992).
99. M. C. Amann, "The effect of spatial correlation on the linewidth broadening in tunable laser diodes", *IEEE J. Quantum Electron.* **QE-29**(6), 1799-1804(1993).
100. M. C. Amann and B. Borchert"Spectral linewidth of tunable twin-guide laser diodes", J. Electron.&Commun., **46**(2), 63-72(1992).
101. M. Hamada, E. Yamamoto, K. Suda, S. Nogiwa and T. Oki, "Narrow linewidth characteristics in tunable twin-guide distributed feedback laser diodes", *Jpn. J. Appl. Phys., Part 2*, **31**(11A), L1552-5(1992).
102. L. Esaki, "Semiconductor superlattices and quantum wells", *Proc. 17th Int. Conf. on The Physics of Semiconductors*, San Francisco, 1984. Eds. J. D. Chadi and W. A. Harrison,

p473(Springer, New York, 1985)
103. D. S. Chemla and D. A. B. Miller, "Room temperature excitonic nonlinear optical effects in semiconductor quantum well structures", *J. Opt. Soc. Am., B*; **1**, 1155-73(1985).
104. D. S. Chemla and D. A. B. Miller and P. W. Smith, "Nonlinear optical properties of GaAs/AlGaAs multiple quantum well material: Phenomena and applications", *Opt. Eng.*, **24**(4), 556-64(1985).
105. D. A. B. Miller, D. S. Chemla, T. C. Damen, A. C. Gossard, W. Wiegmann, T. H. Wood and C. A. Burrus, "Bandedge electroabsorption in quantum well structures: The quantum-confined Stark effect:, *Phys. Rev. Lett.*, **53**, 2173-7(1984).
106. D. A. B. Miller, D. S. Chemla, T. C. Damen, A. C. Gossard, W. Wiegmann, T. H. Wood and C. A. Burrus, "Electric field dependence of optical absorption near the bandgap of quantum well structures", *Phys. Rev., B*, **32**, 1043-60(1985).
107. D. A. B. Miller, D. S. Chemla, D. J. Eilenberger, P. W. Smith, A. C. Gossard and W. Wiegmann, *Appl. Phys. Lett.*, **42**, 925(1983).
108. T. Ishibashi, S. Tarucha and H. Okamoto, in *Proceedings of the International Symposium on GaAs Related Compounds*, Inst. Phys. Conf. Ser., **63**, 587(1981).
109. S. W. Kirchoeefer, N. Holonyak, K. Hess, D. A. Gulino, H. G. Drickamer, J. J. Coleman and P. D. Dapkus, *Appl. Phys. Lett.*, **40**, 821(1984).
110. D. A. B. Miller, D. S. Chemla and S. Schmitt-Rink, "Relation between electroabsorption in bulk semiconductors and in quantum wells: The quantum confined Franz-Keldysh effect", *Phys. Rev., B*, **33**, 6976-82(1986).
111. M. K. Chin, "Comparative-analysis of the performance limits of Franz-Keldysh effect and quantum-confined Stark effect electroabsorption wave-guide modulators", *IEE Proc.-Optoelectronics* **142**(2), 109-14(1995)
112. D. Campi, C. Cacciatore, H.C. Neitzert, C. Rigo and C. Coriasso, "Evaluation of wavefunction coherence length in a waveguide structure embedding a InGaAs/InP short periode superlattice", *Superlattice and Microstructures*, **14** (4), 253-6(1993).
113. L. L. Chang, L. Esaki, W. E. Howard, R. Ludeke and G. Schul, *J. Vac.Sci. Technol.*, **10**, 655(1973).
114. Y. C. Chan and K. Tada, " A study on electroabsorption effects in coupled wuantum wells", *Jpn. J. Appl. Phys., Part 1*, **32**(1B), 536-9(1993)
115. E. E. Mendez, F. Agllo-Rueda, J. M. Hong, *Phys. Rev. Lett.*, **60**, 2426(1988).
116. B. Pezeshki, S. M. Lord, T. B. Boykin and J. S. Harris, "GaAs/AlAs quantum-wells for electroabsorption modulators", *Appl. Phys. Lett.*, **60**(22), 2779-81(1992).
117. S. Cheung, F. Jain, R. Sacks, D. Cullen, G. Ball and T. Grudkowski, "High-contrast Fabry-Perot optical modulator using quantum-confined Stark effect tuning in InGaAs-GaAs multiple-quantum-well cavity", *Appl. Phys. Lett.*, **63**(3), 296-8(1993).
118. O. Zia, P. K. Bhattacharya, J. Singh, T. Brock, "Voltage tunable multiple-quantum-well distributed feedback filter with an electron-beam written schottky grating", *J. Appl. Phys.*, **76**(4), 2550-2(1994).
119. B. C. Cavenett, S. Y. Wang and K. A. Prior "Semiconductor modulators and optical switches", *Phys. Status Solidi B*; **187**(2), 347-53(1994).
120. N. T. Pelekanos, B. Deveaud, P. Gravey, J. M. Gerard, J. Hebling and J. Kuhl, "Optically

produced local spacecharge field in a quantum heterostructure - Towards an all-optical thin-film photorefractive device", *Optical Materials*, **4**(2-3), 358-61(1995).

121. H. Okamoto, "Semiconductor quantum well structures for optoelectronics-Recent advances and furture prospects", *Jpn. J. Appl. Phys., Part 1,* **26**, 315-30(1987).

122 Y. Kan, H. Nagai, M. Yamanishi and I. Suemune, "Field effect on the refractive index and absorption coefficient in AlGaAs quantum well structures and their feasibility for electrooptic device applications", *IEEE J. Quantum Electron.* **QE-23**, 2167-80(1987).

123. H. Nagai, M. Yamanishi, Y. Kan and I. Suemune, "Field-induced modulations of refractive index and absorption coeffient in a GaAs/AlGaAs quantum well structure", *Electron. Lett.*, **22**, 888-9(1986).

124. H. Yamamoto, M. Asada and Y. Suematsu, "Electric field induced refractive index variation in quantum-well structure", *Electron. Lett.*, **21**, 579-580(1985).

125. Y. L. Lam and J. Singh, "Carrier thermalization by phonon absorption in quantum-well modulators and detectors", *IEEE J. Quantum Electron.* **QE-31**(5), 923-6(1995).

126 T. Wolf, K. Drogemuller, B. Borchert, H. Westermeier, E. Veuhoff and H. Baumeister, "Tunable twin-guide lasers with flat frequency-modulation response by quantum confined Stark effect", *Appl. Phys. Lett.*, **60**(20), 2472-4(1992).

127. J. Langanay, E. Gaumont-Goarin, J. Y. Emery, C. Labourie, J. G. Provost, C. Starck, O. Le Gouezigou and D. Lesterlin, "High FM bandwidth of DBR laser including butt-jointed electro-optical wavelength tuning sections", *Electron. Lett.*, **30**(4), 311-2(1994).

2. Device Principles and Design

Introduction

As we reviewed above, using QCSE as the tuning mechanism in a monolithic tunable laser is very attractive and some quite encouraging experimental results have been obtained from a few pioneering tunable laser device experiments. As there are still so many aspects left to be explored in this area, a more systematic study is required. Our objective therefore is firstly to design and fabricate a monolithic semiconductor laser using the QCSE tuning mechanism, having a flat FM response suitable for use in OFM and related systems and secondly from an evaluation of its performance design structures suitable for ultra-fast tuning.

2.1. Laser tuning principles and the tuning by QCSE

As discussed in Section 1, laser tuning is achieved by changing the effective length of the optical path within the optical resonator. We present the principle here in more detail.

2.1.1 Laser tuning principle

We consider the case of a FP resonator which consist of two cleaved facets and a uniform cavity with refractive index n, as shown in Fig.2.1. In almost all monolithic tunable lasers, the change of optical path length is achieved by changing the refractive index of the whole cavity or part of the

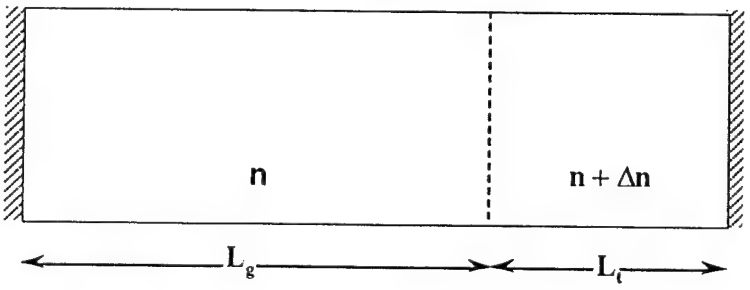

Fig.2.1 The tuning principles of a FP cavity.

cavity. Let us consider a general and simple case where part of the cavity (with length Lt as the tuning part) is used as the tuning section, and the other part (with length Lg as the gain part) retaining a constant refractive index n, thus corresponding to the case of two-section FP tunable laser. When the laser is tuned, the refractive index in the tuning section is shifted by Dn. In a tunable laser, the lasing condition is firstly, that the optical gain in the cavity should at least balance the cavity loss, i.e. the transparency condition, and secondly, the allowed oscillation wavelength should satisfy the standing wave condition, that is the optical path length is equal to an integer number of half wavelengths, or

$$nL_g + (n+\Delta n)L_t = m\lambda/2 \qquad (2.1)$$

where m is an integer and referred to as the mode number. From above, we see when Δn changes, m or λ also changes to follow it. If m remains unchanged, λ can follow the change of Δn continuously, until the optical path change $\Delta nL_t=\lambda/2$, and the oscillation occurs at (m+1) mode. This is the mode jumping case. When tuning is continuous with no mode jumping (m keeps constant) before tuning

$$nL_g + nL_t = m\lambda_0/2 \qquad (2.2)$$

After refractive index changes Δn,

$$nL_g + (n+\Delta n)L_t = m\lambda_1/2 \qquad (2.3)$$

The wavelength shift $\Delta\lambda=\lambda_1-\lambda_0=\lambda_0\Delta nL_t/n(L_g+L_t)$ (2.4)

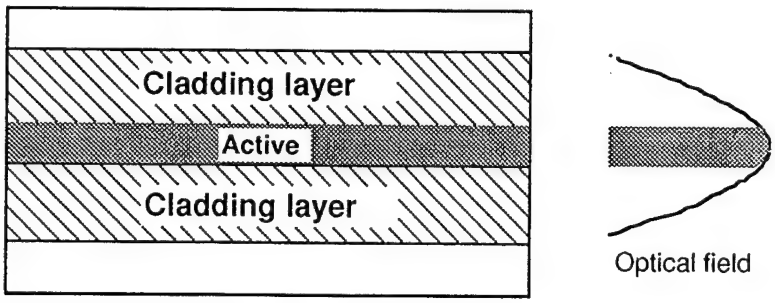

Fig.2.2 Schematic diagram shows the confinement factor Γ.

For more practical case, the physical dimensions of the cavity are finite in both transverse and lateral directions, and the changes of the refractive index generally only happen within the active region as the carriers are confined within it, but the optical field is extended beyond this region. Therefore, the refractive index change in this region affects the cavity refractive index through confinement factor Γ which represents the fraction of optical energy confined within the active region, as shown by Fig.2.2. The effective refractive index change Δn should be substituted by $\Gamma\Delta n_a$ in (2.1) through (2.4), where Δn_a is the refractive index change in active layer, and we have

$$\Delta\lambda=\lambda_1-\lambda_0=\lambda_0\Gamma\Delta n_a L_t/n(L_g+L_t) \qquad (2.5)$$

$$\Delta\lambda/\lambda_0=\Gamma\Delta n_a L_t/n(L_g+L_t) \qquad (2.6)$$

The allowed optical path change before mode jumping is

$$\Gamma\Delta n_a L_t < \lambda_0/2 \qquad (2.7)$$

$$m=2n(L_g+L_t)/\lambda_0 \qquad (2.8)$$

$$\therefore \quad \Delta\lambda_{max}=\lambda_0^{\,2}/2n(L_g+L_t) \qquad (2.9)$$

is the maximum tuning range before mode jumping. It is approximately the mode spacing if the refractive index variation with wavelength is neglected. For a 850 nm laser with n=3.6 and cavity length 500 μm, the maximum continuous tuning range is 0.2nm.

The variation of refractive index can be realised by carrier injection or by field induced QCSE. The refractive index change due to carrier induced effect is less sensitive to wavelength,[1,2] therefore, tuning is smooth in a relatively wide range. For field induced QCSE, which is we are interested in, it is necessary to check its tuning property in more details.

2.1.2. Wavelength tuning by QCSE

Fig.2.3 is the calculated absorption and refractive index change due to QCSE for an 8nm QW structure. From the curve, it is seen that corresponding to the absorption peak at a certain electric field, there is a negative maximum refractive index change. Both the absorption and refractive index change are seen to be a sensitive function of wavelength. For operation close to the exciton absorption peak the refractive index change is accompanied by a large change in absorption. In a monolithic tunable laser, if the tuning section shares the same cavity with gain section, the large absorption and the large variation of absorption with field mean that the lasing threshold condition may be changed during tuning, this is in general not desirable.

Alternatively, there is a relatively smooth positive refractive index change with wavelength at the red side of the exciton peak where the absorption is also small, which seems quite suitable for use in a tunable laser even though the refractive index change is smaller. This is the wavelength region of interest for our laser.

2.2. Device design

In order to develop a monolithic QCSE tuned laser, the following questions must be answered.

1. What laser structure should be chosen?
2. How should the tuning section be incorporated with the gain section, with provision for reverse bias?
3. How will tuning be achieved?

2.2.1. The choice of laser structure

There are some essential requirements for a laser used in a coherent system, such as stable mode behaviour and power output, single longitudinal mode and narrow linewidth. For different coherent systems, the specific requirements for these parameters are somewhat dependent on the modulation used (i.e. amplitude shift keying or ASK, frequency shift keying or FSK, or phase shift keying . PSK), the coherent detection mechanism (i.e. heterodyne or homodyne) and the electrical demodulation technique (synchronous or nonsynchronous)[3]. For most applications, laser linewidth less than 10MHz is essential,[4] and ideally less than 1 MHz. Single longitudinal mode

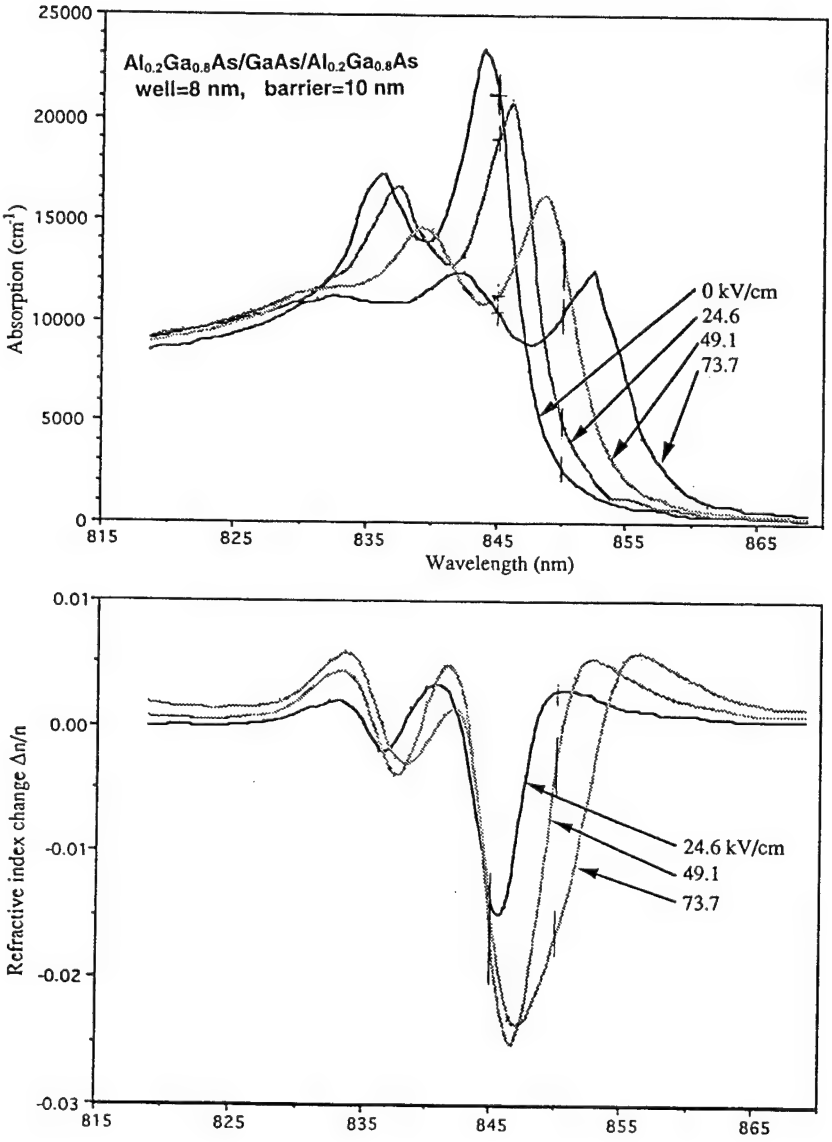

Fig. 2.3 The absorption and refractive index change variation with wavelength under different fields for a AlGaAs/GaAs QW structure. Index changes reference to field=0.

working is very important and is the essential requirement for use in a coherent system. Mode suppression ratio (MSR) generally should be 20 dB or better.

As all lasers developed so far are based on essentially three types of structure: Fabry-Perot, DBR and DFB, it is necessary to compare the mode behaviour of the lasers based on these structures. Since the aim of our study is to investigate the prospect of fast tunable lasers with flat FM response by using QCSE as the tuning mechanism, it will be more practical if we choose the simplest structure which gives reasonable mode suppression and linewidth to enable our investigation to be carried out. Therefore, it is also necessary to look into the processing difficulties for each of the structure.

(i) Mode behaviour comparison of FP, DBR and DFB

Spectral linewidth is associated with the lasing process. It is a fundamental consequence of the spontaneous emission process due to its random nature. Each spontaneously emitted photon changes the optical phase by a random amount. This phase noise affects the phase of the optical field. A change in phase leads to an associated frequency shift. In addition random spontaneous emission and intensity noise cause fluctuation in carrier populations, which leads not only to the change of optical gain, but also the refractive index. These changes also lead to lasing frequency shift. Therefore, physically, spontaneous emission and carrier population fluctuation decide the linewidth of a laser. The linewidth of a single longitudinal mode under CW operation is a manifestation of phase fluctuations occurring inside a laser. Theoretically, the FWHM linewidth of an optical spectrum f for a single mode laser can be written as:[5,6]

$$\Delta f = \frac{V_g \cdot h\nu \cdot n_{sp} \cdot G}{8\pi \cdot P} \cdot (\alpha_i + \alpha_m) \cdot (1 + \alpha^2) \qquad (2.1)$$

where V_g is the group velocity (ratio of photon flux to photon density), $h\nu$ is the photon energy at the main mode, n_{sp} is the spontaneous emission factor, G is the gain, P is light output, α_i is the internal waveguide loss per unit length, α_m is the mirror loss per unit length and α is the linewidth enhancement factor, which is defined as:[7,8]

$$\alpha = -2\kappa_0 \frac{\partial n / \partial N}{\partial G / \partial N} \qquad (2.2)$$

the ratio of refractive index change with carrier density to differential gain change with carrier density, where κ_0 is the vacuum wave number ($=2\pi/\lambda$). It is dependent upon material composition, device structure and operating wavelength. For MQW structure lasers, α is smaller than that in double heterostructure laser, [9] resulting several times smaller linewidth.[9,10] Therefore, we should certainly use an MQW structure as the active layer, which is completely compatible with the requirement of QCSE. As the effective mirror loss per unit length decreases when the cavity length increases, extending cavity also reduces the linewidth. This is the reason that external cavity laser has smaller linewidth. It is also seen that the linewidth is inversely proportional to the output power.

The influence of structural differences on linewidth is mainly reflected by the structural dependence of spontaneous emission factor n_{sp}, cavity loss $\alpha_i+\alpha_m$, and the linewidth enhancement factor α. For FP cavity lasers, the internal loss α_i mainly comes from free carrier absorption and the layer interface scattering,[11] and the mirror loss is due to the radiation escaping from FP cavity because of the finite facet reflectivity. For DBR structure, beside the same cavity loss mechanisms, two additional loss mechanisms may increase the total cavity loss: (i) scattering loss due to grating imperfection and (ii) coupling loss between active and passive (grating) region. [6] For DFB structures, similar cavity loss mechanisms to DBR structures exist, except that the coupling loss is substituted by radiation loss from periodic structures which happens due to higher order Bragg diffraction.[13,14] We can see, for the cavity loss, FP structure is lower than either DBR and DFB structure, and because coupling loss is larger than grating imperfection or radiation loss, DBR structure suffers the biggest cavity loss. On the other hand, for a FP laser, the feedback is provided by facet reflection whose magnitude remains the same for all longitudinal modes. The only mode discrimination in such a laser is provided by the gain spectrum itself. Generally, the gain spectrum is much wider than the longitudinal mode spacing. It is quite different for DBR or DFB lasers where the feedback is strongly wavelength-dependent, resulting in a much narrower cavity gain spectrum compared to the FP structure. Due to this stronger mode discrimination mechanism in DBR and DFB structures, the mode suppression ratio (MSR) of DBR or DFB lasers is larger than that for FP lasers. Since the spontaneous emission factor is related to gain spectrum, FP cavity has larger n_{sp} than DBR or DFB cavity laser due to its broader gain spectrum. [15] As a total effect, there is no obvious big difference among the three structures if we consider only linewidth. The narrow linewidth is totally dependent on specific device structure, and may be quite different even with the same structure or from the same wafer. For example, due to the sensitivity of DFB laser performance not only to the facet reflectivity but also to the grating phases at the facets, many laser characteristics, including linewidth, vary from device to device [16].

Experimentally, much progress has been achieved in the fabricating techniques in obtaining smaller linewidth of FP, DBR and DFB lasers. Table 2.1 list some typical results reported for these lasers.

Table 2.1 The best results achieved with FP DBR and DFB lasers

Cavity	Laser structure	Linewidth	MSR	Output power	Reference
F-P	MQW ridge waveguide	~2.5 MHz		10 mW	[17]
	Metal cladding MQW ridge waveguide	2~4 MHz	≥20 dB	20~10 mW	[18]
DBR	MQW ridge waveguide	~3.2 MHz	≥30 dB	1.5 mW	[19]
	MQW ridge waveguide	~560 kHz			[20]
	MQW	~743 kHz	≥40 dB		[21]
DFB	MQW ridge waveguide	~1 MHz	≥40 dB	20~30 mW	[22]
	Extended cavity	~170 kHz			[23]
	MQW ridge waveguide	~270 kHz	≥30 dB	13.5mW	[24]

From these results, we can see very narrow linewidth has been achieved by using DFB or DBR cavities. This is mainly because most of the effort has been concentrated on the DBR and DFB laser in the latest decade due to their more advanced performance over FP lasers in practical applications, but it is also quite possible to reduce the linewidth of FP cavity laser further through improving structure design and epitaxy growth techniques. The main advantage of DBR and DFB laser are their high MSR and stable mode behaviour.

(ii) Fabrication of FP DBR and DFB lasers

The FP cavity laser is very simple in fabrication. It requires only one step of epitaxy growth and several simple processing steps which are completely compatible with general semiconductor processing, no difficult process steps are involved. In contrast, DBR or DFB cavity lasers require the fabrication of a Bragg grating which is crucial to the laser performance and can be done only by electronic beam lithography or holographic technique, and at least two steps of epitaxy growth which is normally difficult to achieve with good quality, making their fabrication very difficult. The use of re-growth processes in epitaxy increases the difficulty in obtaining good quality MQW structures. In order to avoid our study being blocked by poor re-growth quality or the difficult of grating fabrication, we chose an FP cavity for our laser structure in the first stage of the study. Upon the success of the fast tuning study, the methods and conclusions can be easily transferred to more advanced DBR or DFB cavity laser structures.

The ridge waveguide structure is the most popular laser structure no matter what the cavity formation due to its simple fabrication processing and good lasing performance.[25,26] We chose also the ridge waveguide as our laser structure.

Although most optical communication systems nowadays use 1.3 and 1.55m laser systems, based on InP semiconductor, as a generalised research, we decided to use more general and popular GaAs semiconductor for our study. It also offers convenient interface wuth GaAs monolithic microwave integrated circuits (MMICs) This means the our lasing wavelength is around 850 nm.

In conclusion, cavity formation (FP, DBR or DFB) has no direct important affect on laser spectral linewidth, even though very narrow linewidth has been achieved by DFB and DBR lasers. For FP cavity laser, linewidth less than 10 MHz and MSR 20 dB, which are the basic requirements for our study, are readily achievable. FP cavity ridge waveguide laser is the simplest one in fabrication processing and provides us with the highest possibility to achieve a good performance laser and enable us carry out the fast tuning study on it. As a consequences, we chose GaAs based FP cavity ridge waveguide laser structure as our laser structure in our study.

2.2.2. The incorporation of gain and tuning sections

There are at least three methods of combining gain and tuning sections in a tunable laser: single cavity, multi-section configuration; separate but coupled cavity, multi-section as in C^3 laser and the last, twin-guide configuration. Since in cleaved-coupled cavity configuration, the tuning section

can only function as a mode selection element, it is not of interest. We mainly consider single cavity and twin guide cavity configurations.

(i) The tuning comparison of single cavity and twin guide cavity

As we pointed out in Section 1, the advantage of the twin-guide tunable laser is that it allows independent control of tuning and lasing performance and avoids the output power variation which is normally associated with single cavity tunable lasers. Fig.2.4 shows the optical field distribution along the transverse (perpendicular to the p-n junction plane) direction for these two configurations. The continuous wavelength shift before mode jumping is : $\Delta\lambda=\Gamma\Delta n\lambda_0 L_t/(L_a+L_t)n$ for the single cavity case, and $\Delta\lambda=\Gamma\Delta n\lambda_0/n$ for the twin guide case. The confinement factors in the two cases correspond respectively to the shadowed area in Fig.2.4. Obviously, due to the existence of the thick central isolation layer the confinement factor in the twin guide cavity is quite small compared to that of the single cavity. Considering the factor of $L_t/(L_a+L_t)$, we can conclude that as far as tuning efficiency is concerned, the twin-guide cavity has no advantage over the single cavity configuration. Moreover, there is more freedom to control the tuning range through change in the factor of $L_t/(L_a+L_t)$, even though the very strong wavelength dependence of QCSE limits the possible tuning range. On the other hand, the twin-guide cavity normally requires re-growth and more complicated fabrication processing which is undesirable, therefore the single cavity, two-section configuration is more suitable for our study.

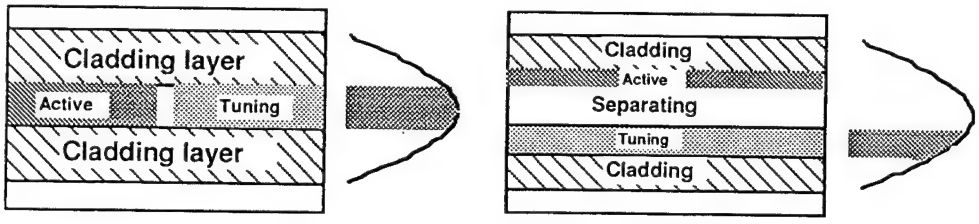

Fig.2.4 The tuning comparison of single cavity and twin-guide schemes.

(ii) Isolation method between sections

In order to achieve a large electric field within the MQW layer, the tuning section must be reverse biased. Therefore, it is important to adopt a proper method to achieve good isolation between the gain and tuning sections. One of the most simple methods is by using ion implantation, as shown in Fig.2.5.

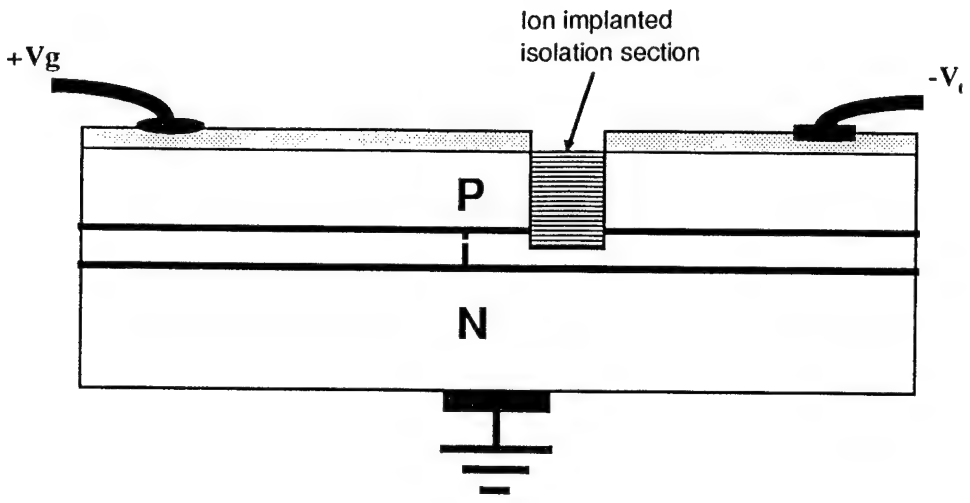

Fig.2.5 Ion implantation to achieve isolation between gain and tuning section.

Proton bombardment is found to raise the resistivity of GaAs significantly due to ion induced defect traps the carrier.[27,28] Many other ions, such as O^+, F^+, B^+, N^+, are all found to transfer the implanted region into semi-insulating.[27] Among them, H^+ and O^+ are the most suitable candidates for our purpose. The ion implanted region usually has very high optical absorption, which is not desired for our study. However, upon a proper annealing after implantation, the absorption increase of the implanted region could be annealed out completely in the case of proton bombardment,[29] and nearly completely annealed out (>90%) in the case of O^+ implantation. The difference of H^+ and O^+ implantation is that in an H^+ implanted sample, optical absorption reduction upon annealing is achieved at the expense of reduced resistivity, but in an O^+ implanted sample, the resistivity reducing with the reduction upon annealing is quite gradual, and reaches a saturation value since in O^+ implanted isolation both ion induced defect and oxygen doping effects occur,[27,30] instead of only ion induced defect effect in the proton bombarded case.

The advantage of H^+ implantation is its large projected range, that is , even under low implanting energy, the H^+ can still have large penetration depth.

Therefore, we keep both schemes as candidates for ion implanting isolation in our study.

In conclusion, a single cavity ridge guide with multi-section configuration is the structure we have chosen for our tunable laser study, and ion implantation is a convenient method to achieve good isolation between the forward biased gain section and the reverse biased tuning section. H^+ and O^+ are the potential candidates we have chosen to realise the implantation isolation.

2.2.3. Tuning by using QCSE and the band gap shift

As we discussed in Section 2.1.2, the refractive index change due to QCSE is very sensitive to the operating wavelength. As shown in Fig.2.3, the wavelength corresponding to maximum refractive index change for a certain electric field deviation corresponds to the maximum absorption. This

means, when the tuning section is tuned, the output power, even the threshold condition is also changed, which is certainly not what we desired. Fortunately, when the gain section reaches threshold condition, the high carrier density results in band gap reduction, [31] and the lasing wavelength is about 10nm longer than the exciton peak. This means by sharing the single cavity, the tuning section is working at a longer wavelength where the absorption may be small, but the refractive index change is also smaller. In order to optimise both lasing and tuning performance, it is necessary to find some way to shift the exciton peak to higher energy in order to achieve lowest absorption loss and reasonable refractive index change.

There are several methods for doing this. Impurity induced band gap disordering by thermal diffusion of impurity species [32] or by ion implantation into the active layer [27,33] are examples of these methods. [34] Impurity-free vacancy [35,36] diffusion (IFVD) is the most widely used and more convenient method for most applications. In this approach, an insulator film of SrF_2 is deposited over the region where no band gap shifting is required, and then SiO_2 is deposited over the whole wafer. After high temperature (900 C) and short time (30 seconds) annealing, the region covered by only SiO_2 obtains obvious blue shift which is proportional to the annealing temperature and time, and the region covered first by SrF_2 and then by SiO_2 only shows very small band gap shift. The physical reason behind this is the Ga out-diffusion into the SiO_2 capping layer and Al in the nearby barrier has a good possibility of diffusing to the QW to occupy the Ga vacancy, therefore the well depth and width reduces resulting in exciton peak shifts to higher energy.

From the above analysis, we have seen that the IFVD technique is a suitable method to achieve blue shift in the tuning section, which could be an important technique needed in our study.

2.3 Conclusion

In this Section, we have presented the essential tuning principles for tunable lasers and the use of QCSE as the tuning mechanism. It is seen that for QCSE, the tuning performance is very wavelength dependent. The linewidth and MSR of FP, DBR and DFB cavity laser were compared and analysed. Despite the good linewidth and MSR achieved for DBR and DFB lasers, in order to concentrate our study on fast reverse biased tuning itself and avoid the difficult fabrication of DBR and DFB laser, we choose an FP cavity laser as the basis of our tunable laser study. Compared to DBR or DFB laser, the FP laser is comparable in linewidth, and can readily achieve MSR >20dB. A ridge waveguide laser structure is chosen to be our laser structure. The single cavity, two-section tunable laser configuration is a suitable system for our study. Ion implantation is to be used as the isolation method between the forward biased gain section and the reverse biased tuning section. IFVD technique is the most suitable technique to achieve required blue shifts in the tuning section.

2.4 References

1. G. H. B. Thompson, "A theory for filamentation in semiconductor lasers including the dependence of dielectric constant on injection carrier density", *Opt. Electronics*, **4**, 257-310(1972).

2. E. Garmire, *Integrated Optics*, Springer, New York, 1975.
3. M. Shikada, I. Mito, K. Emura, S. Murata, K. Komatsu, K. Kaede and K. Minemura, "Optical devices for coherent optical fibre transmission systems", in *Conf. Rec. GLOBCOM'87* (Tokyo, Japan), **Vol.1,** 694-8(1987).
4. I. W. Oh and H.R.D. Sunak, "Measurement of the spectral linewidth of semiconductor lasers for use with coherent optical communication systems", *IEEE Trans. on Instru. and Meas.*, **IM-36**(4), 1054-9(1987)
   I. W. Oh and H.R.D. Sunak, "measurement of the spectral linewidth of semiconductor lasers for use with coherent optical communication systems", *Conf. Proc. of IEEE Instrumentation and Measurement Technology Conference.*, Boston, MA, USA, 27-29 Apr 1987, pp.273-277(1987)
5. C. H. Henry, "Phase noise in semiconductor lasers", *J. Lightwave Technol.* **LT-4**, 293-311(1986).
6. C. H. Henry, "Theory of the linewidth of semiconductor lasers", *IEEE J. Quantum Electron.* **QE-18**(2), 259-64(1982).
7. C. Harder, K. Vahala and A. Yariv, *Appl. Phys. Lett.*, **42**, 328(1983).
8. M. Osinski and J. Buus, *IEEE J. Quantum Electron.* **QE-23**, 8(1987)
9. Y. Arakawa and A. Yariv, "Theory of gain, modulation response, and spectral linewidth in AlGaAs quantum well lasers", *IEEE J. Quantum Electron.* **QE-21**, 1666-74(1985).
   Y. Arakawa and A. Yariv, *IEEE J. Quantum Electron.* **QE-22**, 1887(1986).
10. M. Aoki, K. Uomi, T. Tsuchiya, S. Sasaki, M. Okai and N. Chinone, *IEEE J. Quantum Electron.* **QE-27**, 1782(1991).
11. H. C. Casey, Jr. and M. B. Panish, *Heterostructure lasers*. New York: Academic Press, 1978.
12. Y. Suematsu, S. Arai and K. Kishino, *J. Lightwave Technol.* **LT-1**, 161(1983).
13. W. Streifer, R. D. Burnham and D. R. Scifres, *IEEE J. Quantum Electron.* **QE-12**, 737(1976).
14. R. F. Kazarinov and C. H. Henry, *IEEE J. Quantum Electron.* **QE-21**, 138(1985).
15. C. H. Henry, *J. Lightwave Technol.* **LT-4**, 288(1986).
16. J. Glinski and T. Makano, *IEEE J. Quantum Electron.* **QE-23**, 849(1987).
17. Y. Matsushima, K. Utaka and K. Sakai"Narrow spectral linewidth of MBE-grown GaInAs/AlInAs MQW lasers in the 1.55 m range", *IEEE J. Quantum Electron.* **QE-25**(6), 1376-80(1989).
18. Garrett/mcrwg B. Garrett and R. W. Glew, *Electronics Letters*, **23**(8), 371-373(1987)
    We also measured the linewidth of the same laser, the line width is less than 2.5 MHz when output power approaches 20mW, and nearly 4 MHz when output power less than 10 mW.
19. M. Takahashi, Y. Michitsuji, M. Yoshimura, Y. Yamazoe, H. Nishizawa and T. Sugimoto, *IEEE J. Quantum Electron.* **QE-25**, 1280(1989).
20. F. Kano, M. Nakano, M. Kukuda, Y. Kondo, Y. Tohmori and K. Oe, *Electron. Lett.*, **25**, 709(1989).
21. J.I. Shim, T. Nomaguchi, K. Kudo ans S. Arai, *Electron. Lett.*, **28**, 741(1992).
22. dutta p381/116 M. Kitamura, H. Yamazaki, T. Sasaki, N. Kida and I. Mito, *IEEE Photon. Technol. Lett.*, **3**, 305(1991).

23. M. Okai, T. Tsuchiya, K. Uomi, N. Chinone and T. Harada, *IEEE J. Quantum Electron.* **QE-27**, 1767(1991).
24. M. Aoki, K. Uomi, T. Tsuchiya, S. Sasaki, M. Okai and N. Chinone, *IEEE J. Quantum Electron.* **QE-27**, 1782(1991).
25. R. F. Kazarinov, C. H. Henry and R. A. Logan, *J. Appl. Phys.*, **53**, 4631(1982).
26. G. P. Agrawal, *IEEE J. Quantum Electron.* **QE-23**, 860(1987).
27. S. J. Pearton, "Ion implantation in III-V semiconductor technology", *Int. J. Modern Physics B*, **7**(28), 4687-4761(1993).
28. P. N. Favannec and D. Diguet, "Electrical properties of proton bombarded GaAlAs", *Appl. Phys. Lett.*, **23**, 546-7(1973).
29. J. C. Dyment, J. C. North and L. A. D'asaro, "Optical properties and electrical properties of proton bombarded p-type GaAs", *J. Appl. Phys.*, **44**, 207-13(1973).
30. E. V. K. Rao, "Optical properties of oxygen implanted GaAs", *Physica Status Solidi A*, **33**(2), 683-90(1976).
31. F. Stern, *J. Appl. Phys.*, **47**, 5382(1976).
32. R. L. Thornton, R. D. Burnham, T. L. Paoli, N. Holonyak, Jr. and D. G. Deppe, "Opto-electronic structures fabricated by impurity induced disordering", *J. Cryst. Growth*, **77**, 621-28(1986).
33. T. Hirata, M. Maeda, M. Suehiro and H. Hosomatsu, "GaAs/AlGaAs GRIN-SCH-SQW DBR laser diodes with passive waveguide integrated by compositional disordering of the quantum well using ion implantation", *Jpn. J. Appl. Phys., Part 1*, **29**(6), L961-3(1990).
34. R. L. Thornton, R. D. Burnham, N. Holonyak, Jr., J. E. Epler and T. L. Paoli, "Impurity induced disordering of heterojunction interface: phenomenology and laser device application", *SPIE* **Vol. 797**, *Advanced Processing of Semiconductor Devices*, 177-184(1987)
35. I. Gontijo, T. Krauss, J. H. Marsh and R. M. De La Rue, "Post growth control of GaAs/AlGaAs quantum well shapes by impurity-free vacancy diffusion", *IEEE J. Quantum Electron.* **QE-30**(5), 1189-95(1994).
36. J. H. Marsh, "Quantum well intermixing", *Semicon. Sci. & Technol.*, **8**, 1136-55(1993).

3. Device Fabrication Processing

Introduction

Firstly, a successful monolithic tunable laser relies totally on a successful single longitudinal mode, narrow linewidth and CW working laser. The epitaxial growth quality, especially the MQW layer quality, is the key factor affecting the laser performance. It is proved by many researchers that MOCVD (or equivalently MOVPE) technology can provide the best epitaxial growth for laser applications, therefore, we have chosen atmosphere MOVPE as the epitaxial growth technique for our laser structure. The epitaxial structure is shown in Fig.3.1a, the whole structure is grown between 600-700 °C by MOVPE at III-V Semiconductor Facility in Sheffield. The active layer consists of five 6.9 nm QWs separated by 10 nm thick $Al_{0.3}Ga_{0.7}As$ barriers, and sandwiched between two 100 nm $Al_{0.3}Ga_{0.7}As$ guiding layers, which form the core of the waveguide. The cladding layer consists of two 1 μm AlGaAs layers. After growth, the wafer is checked by photoluminescence. A PL peak of 838 nm is found at room temperature, which corresponds to the MQW exciton peak.

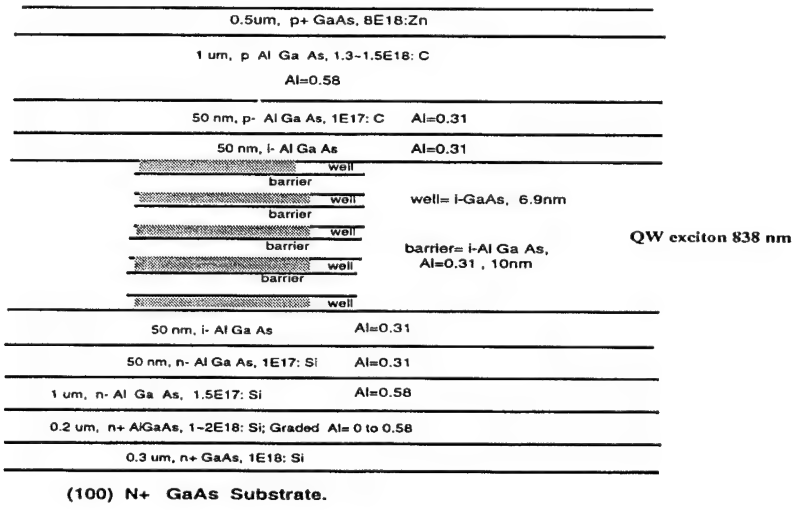

Fig. 3.1a Wafer structure for laser fabrication grown by MOVPE

After the MOVPE growth, the wafer is processed by the optimised processing, which is the subject of this chapter.

It is proved that ridge waveguide lasers can give very good lasing performance.[1] Due to its processing simplicity and good controllability, we have chosen the ridge waveguide structure as our laser structure. Fig.3.1b is the main procedures for processing the 5 μm ridge waveguide

Fabry-Perot laser diode. The whole fabrication process consists of eleven steps which can be summarised as follows:

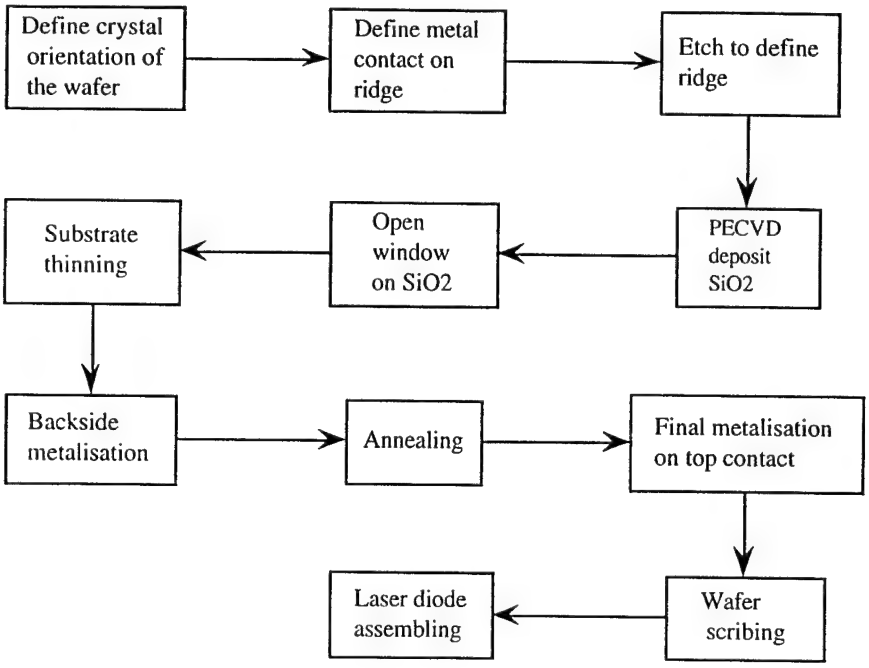

Fig. 3.1b The main procedures of ridge waveguide laser diode.

1. *Define crystal orientation:* cutting the wafer into smaller pieces to reveal clear crystal orientation, and photolithography to make marks on wafers as a reference for the followed masks alignment.
2. *Define metal contact on ridge:* lithography and metal(Cr/Au) lift-off to define ridge contact along crystal direction. The contact (3 μm in width) also serves as the first Ohmic contact metal layer.
3. *Etch to define ridge:* lithography and acid etch to reveal 5μm wide ridge and 10 μm wide troughs in each side.
4. *PECVD deposit SiO_2:* insulator film between contact metal and semiconductor.
5. *Open window on SiO_2:* lithography to open 3μm wide line window for second layer metalisation on the top of the first metal layer.
6. *Substrate thinning:* lap down the backside of the wafer by polishing to required thickness.
7. *Back side metalisation:* perform metal deposition on the back of n-substrate, generally Ni/GeAu/Au.
8. *Annealing:* make metal-semiconductor alloy at around 420 ^{0}C to achieve Ohmic contact.
9. *Final metalisation on the top contact:* Ti/Au metals deposition and lift-off as the 2nd layer metal contact on the top of the ridge.
10. *Wafer scribing:* scribe and fracture wafer into laser bars and finally, laser dice.
11. *Laser diode assembling:* mount laser chip on suitable heat sink and bond it by ultrasonic bonding.

3.1. Define crystal orientation

3.1.1. Wafer preparation

Generally, the wafer is cut into smaller pieces for processing. As laser diodes require perfect facets, great attention should be draw to the cutting of the wafer. Use of a diamond knife with a good tip to scribe a short line near the edge of the wafer, and letting it fracture along its own crystal structure by using a middle soft mat and bar, should generally give a perfect lateral face which is perpendicular to the wafer mirror surface.

3.1.2. Wafer cleaning

The following general cleaning procedures are listed as a standard cleaning processing for III-V semiconductor materials.

1. Immerse the wafer in TCE(trico, or trichloroethylene) which is contained in a clean beaker, and place the beaker on a hot plate(~150 ^{0}C) for heating. Let it boil for 5 minutes, and then place it into an ultrasonic water bath for 5 minutes to remove all possible grease away. Change the solvent with fresh TCE, and place in the ultrasonic water bath for another 2 minutes, then
2. Change solvent with acetone, ultrasonic for 5 minutes, and repeat this procedure once more to clean TCE.
3. Change the solvent with methanol to remove acetone, twice.
4. Use IPA for final cleaning, and then blow dry in N_2.
5. Place wafer into a 140 ^{0}C oven for 10 minutes to drive off all solvent. Remove from oven to allow it to cool.

3.1.3. Define crystal orientation

The aim is to make marks on the wafer by using photolithography and wet etch. This is for the convenience of mask alignment in the later steps, and more importantly, to guarantee that the final facets of the laser diode will be perfect crystal surfaces along the crystal structure and perpendicular to the ridge of the waveguide.

1. Spin photoresist on wafer: coat the cleaned wafers with Shipley S1818 or S1813 positive photoresist, spin at a speed 5000rpm for 30 seconds.
2. Soft bake: place wafers on 100 ^{0}C hot plate for 1 minute, or in 100 ^{0}C oven for 20 minutes.
3. Align and expose: using marks mask (Mask 3 of laser masks set as shown in appendix of this chapter). Place the wafer on the stage of mask aligner, carefully adjust the long axis direction of the wafer to the long-axis direction of the patterned mask(Fig.3.2), and expose for 5 seconds.
4. Develop: immerse in 351(Shipley developer):DI water=1:3.5 developer for about 30 seconds for developing, and rinse in DI water to clean developer completely. N_2 blow dry.
5. Hard bake: place wafers on 115 ^{0}C hot plate for 1 minute as the hard bake. Allow it to cool.
6. Pattern etch: immerse wafers in etchant H_2SO_4: H_2O_2 H_2O=1:10:10 for 30 seconds, rinse in large amount DI water, and blow dry in N_2.
7. Remove resist and clean: use acetone→methanol→IPA to remove photoresist and clean wafers.

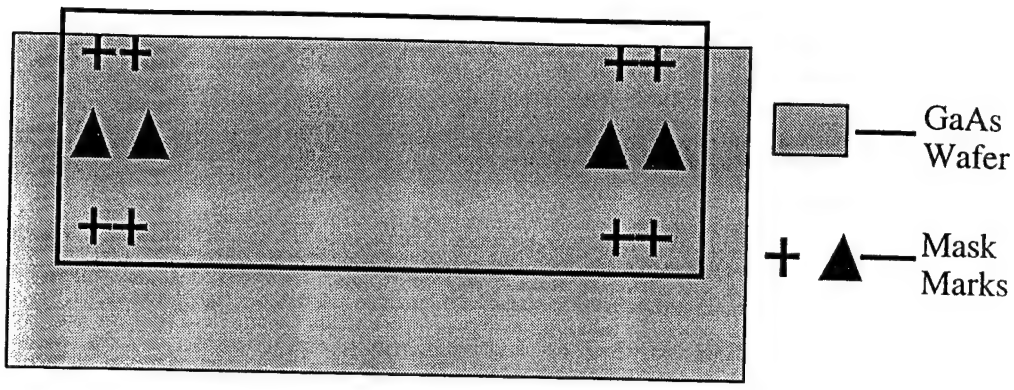

Fig.3.2 Aligning marks along long crystal axis of the wafer.

The marks should be left on the wafer with a depth of 1~2 μm. They serve as the reference for further mask alignment.

3.2. Define metal contact on ridge

By using lithography, Cr/Au metals deposition and metal lift-off, define a 3 μm wide metal contact line on the wafer.

1. Photolithography: after many experiments, we finally arrived at the following procedure which is quite successful in giving us very nice overhanging photoresist profile to fulfil the requirement of metal lift-off.

   spin BPRS-150 positive tone photoresist, 4000rpm, 20 seconds.
   soft bake on hot plate, 90 ^{0}C, 1 minute.
   re-spin S1813, 4000rpm, 20 seconds.
   soft bake again on hot plate, 85 ^{0}C, 1minute
   use ridge mask (Mask 11), align the marks on mask to the marks on wafer, and expose 4 seconds.
   soak in chlorobenzene for 4~5 minutes and blow dry in N_2
   develop for about 60 seconds. in developer and rinse in DI water
   blow dry by N_2

The function of soaking in chlorobenzene is to harden the outermost surface region of the resist[2-4]. Due to diffusion of chlorobenzene into the resist, the region contaminated by chlorobenzene will have slower developing speed comparing to the normal resist which chlorobenzene did not reach. The final resist will have an undercut(overhanging) or vertical profile, as shown in Fig.3.3a.

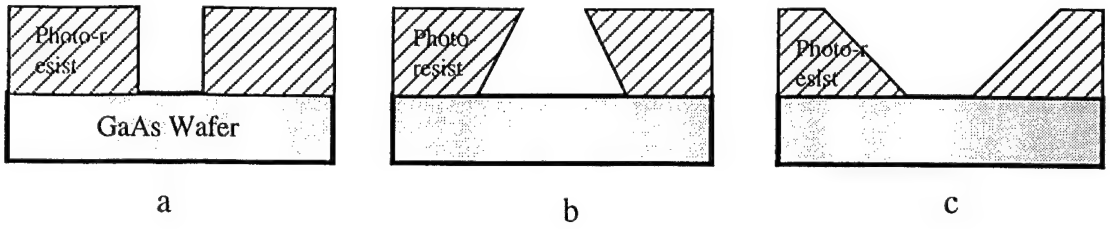

Fig.3.3a. The possible photoresist profile after lithography. **a** is fair and **b** is good for metal lift-off, while **c** is not good as metal covers the entire area of the photoresist.

2. HCl etch: dip the wafers in HCl:DI=1:1 etchant for 30 seconds to remove the outermost surface layer of GaAs in order to make sure of the Cr/Au contact to the real and fresh p^+-GaAs cap layer. Rinse in DI water and blow dry in N_2.
3. Mount wafers on microscope slides by using wax and hotplate or vacuum grease and place them into the vacuum chamber. Pump down the vacuum to $P< 4x\ 10^{-6}$ mbar.
4. Metal deposition: evaporate Cr first, 10~12 nm; then Au , 200 nm

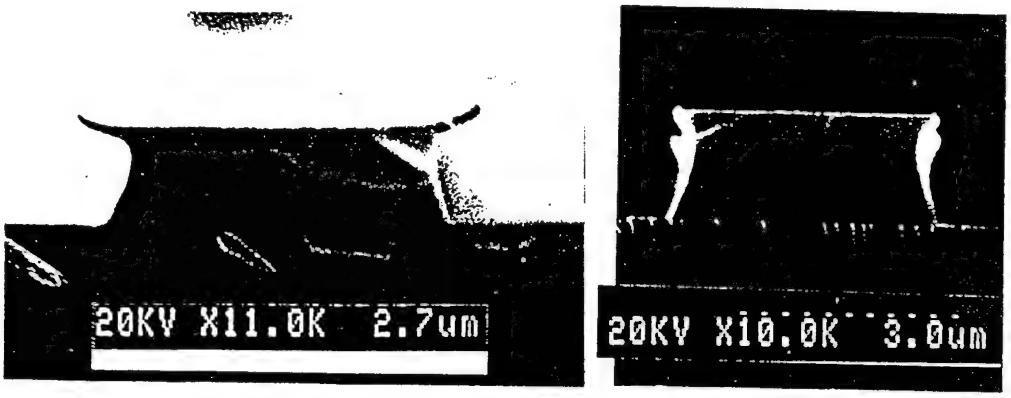

Fig.3.3b. SEM pictures show the photoresist profiles for metal lift-off.

5. Metal lift-off: remove glass slides from vacuum chamber and immerse in acetone. If the cross profile of the photoresist has an overhanging or nearly vertical structure after lithography, as shown in Fig.3.3b, the unwanted metal should be able to leave the wafer easily and a fine metal feature will be left, otherwise, lift-off will not be successful. Using most suitable photoresist, processing conditions and developer to achieve a proper resist profile before perform metalisation.
6. Clean wafers: standard cleaning procedures as described above to clean wafers.

The wafer should now be patterned as show in Fig.3.4.

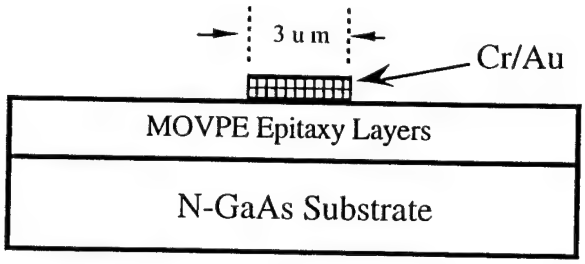

Fig. 3.4. 3um Cr/Au contact above the ridge waveguide.

3.3. Define ridge

By lithography and acid etching, define a 5 μm ridge by etching 10 μm wide troughs on each side of the ridge. One must carefully control the etch depth as it will be crucial for the laser diode performance. Anisotropic and slower etchant are preferred for the purpose of a vertical side wall and a controllable of etch depth. The proper etch depth is crucial in the mode behaviour of ridge waveguide laser, as for this weak index guided laser, lateral mode confinement is determined by the proper depth of the trough.[1] 0.2 ~ 0.4 μm above the core guiding (inner cladding) layer is the most ideal depth. The steps are:

1. Lithography: use resist S1818 and trough etch mask (Mask 4), to open the window for trough etch . Other conditions are the same as in 3.1.3.
2. Hard bake: 115 ^{0}C hot plate for 1 minute, allow to cool.
3. Etch: There are two methods to perform etching. One is wet chemical etching by using H_2SO_4: H_2O_2 :H_2O =1:8:80 etchant, check the etching depth regularly by using an accurate step measuring instrument during etching until the required depth is obtained. The other is reactive ion etching(RIE) which employs plasma CF_4 or $SiCl_4$ to react with III-V materials. The first method can give accurate etch depth and is a quick and simple process whilst the second can give a vertical sidewall but it is difficult to control the required etch depth and is a very time consuming processing.
4. Remove resist by acetone and clean by standard cleaning procedures.

The final ridge is 5 μm wide and the bottom of the troughs should be 0.2~0.4μm above the inner cladding layer, as shown in Fig.3.5.

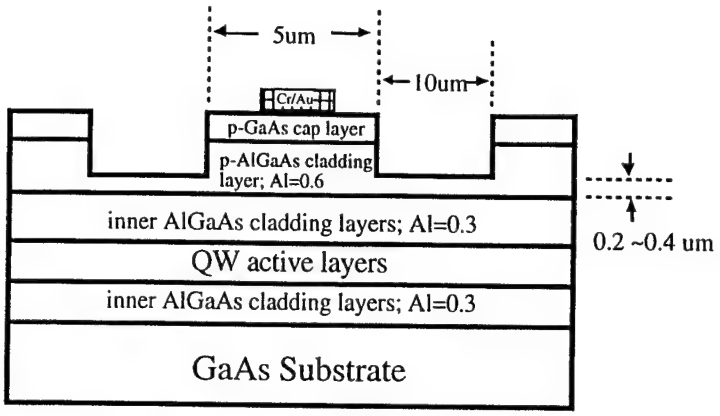

Fig. 3.5. The cross section view after ridge define by wet etching.

3.4. Deposit PECVD SiO_2

By plasma enhanced chemical vapour deposition(PECVD), deposit SiO_2 (or Si_3N_4) as the insulator film between metal layer and semiconductor.

1. Place wafers into PD80 PECVD films depositing system.
2. Deposit condition: Pressure 200 mtorr
   SiH_4 10 sccm
   N_2 35 sccm
   N_2O 70 sccm
   Temperature 300 ^{0}C
   Duration 10 minutes
   RF power 18 W

The final thickness of SiO_2 should be around 200 nm, as shown in Fig.3.6.

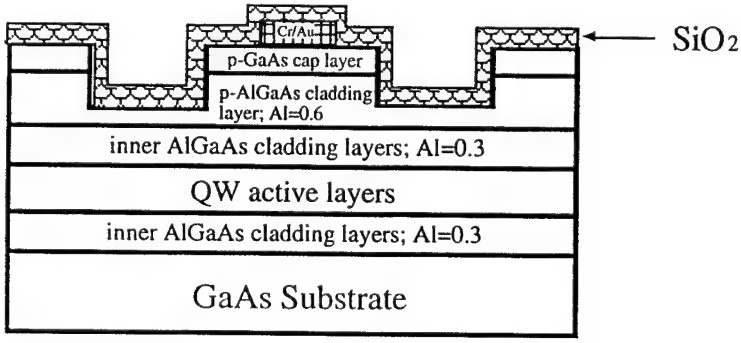

Fig. 3.6. The cross section view after SiO_2 deposition by PECVD.

3.5. Open window on SiO_2

Open 3 μm wide line windows above the ridge metal contact for the second layer metalisation, as shown in Fig.3.7.

1. Lithography: S1818 resist, 3μm ridge mask (Mask 11), other conditions are the same as in 3.1.3.
2. Hard bake: 115 ^{0}C hot plate for 1 minute, allow to cool.
3. SiO_2 etching: immerse in buffered HF until SiO_2 is etched away completely, roughly 2 minutes. Rinse in large amount DI water and blow dry in N_2.
4. Rinse in acetone and blow dry in N_2.

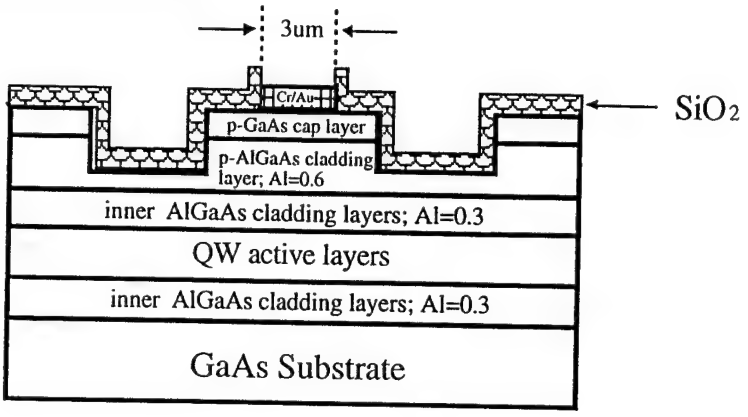

Fig.3.7. The cross section profile after open 3um window on SiO_2.

3.6. Thinning substrate

Lap down the substrate to required thickness by polishing.

1. Mount the wafers face down on coverslips using wax and hotplate, make sure the wafer is parallel to the coverslip, and then mount coverslips on polishing head.
2. Thin to about 80 μm by using 1000 grade carborundum.
3. Remove coverslips from polisher and clean them by hot TCE → cool TCE → acetone → methanol and IPA, blow dry in N_2.

3.7. N-type substrate metalisation

Deposit Ni/GeAu/Au metals to backside of the wafer for Ohmic contact.

1. Mount coverslips on microscope slides by using wax and hotplate or other methods.
2. Place slides into vacuum chamber, and pump down to $P<4\times10^{-6}$ mbar.
3. Deposit first metal layer Ni: 10nm;
   second GeAu alloy: 100nm;
   last Au layer: 200nm;
4. Remove slides from vacuum chamber and dismount coverslips from the microscope slides and wafers from the coverslips.
5. Use standard cleaning procedures to clean wafers. As the wafer is very thin, every precaution should be taken to avoid damaging the wafers.

3.8. Annealing

Place cleaned wafers into a 420 ^{0}C alloying furnace , anneal for 2 minutes in forming gas(10% H_2 and 90% N_2), and then move the wafers out of the furnace. At this temperature, metal-semiconductor(Cr-GaAs and Ni-GaAs) will form a very thin alloy layer with lowered band gap and surface barrier in the near surface layer[5] with low resistivity to serve as the Ohmic contact. The hydrogen in the forming gas will help to reduce the surface dangling bond and surface state density, improving the electrical properties of the contact.

3.9. Final metalisation on top contact

Lithography, metals deposition and metal lift-off to form the 2nd metal layer on the p+ top contact.

1. Mount the wafers face-up on coverslips using photoresist, make sure the wafer is parallel to the coverslip.
2. Lithography: as described in 3.2, using final metalisation mask (Mask 8) to define metal lift-off pattern on wafer.
4. Mount coverslips on microscope slides by using wax and hotplate or photoresist.
5. Place slides into vacuum chamber, and pump down to P<4×10^{-6} mbar.
6. Deposit first metal layer Ti: 40nm;
   second metal Au: 200nm;
7. Remove glass slides from the vacuum chamber and immerse in acetone for metal lift-off. The wafers should also be floated off the coverslips. Rinse wafers in acetone-methanol-IPA and blow dry in N_2.

The wafer now has the structure as shown in Fig.3.8a, Fig.3.8b is the SEM picture of a laser diode.

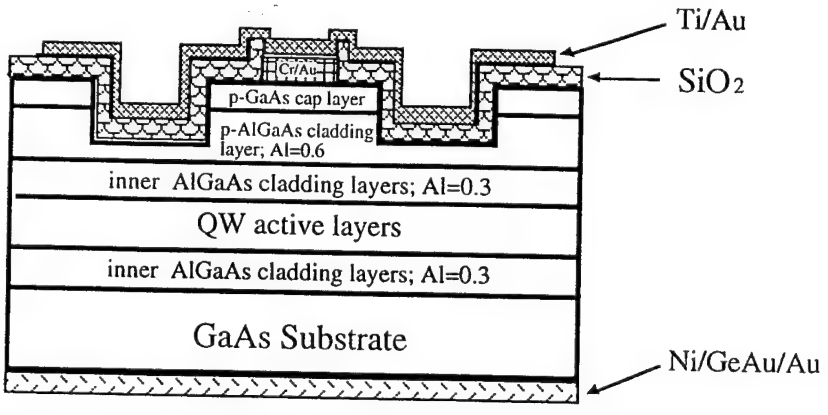

Fig. 3.8a. The cross section profile after final metalisation on top contact.

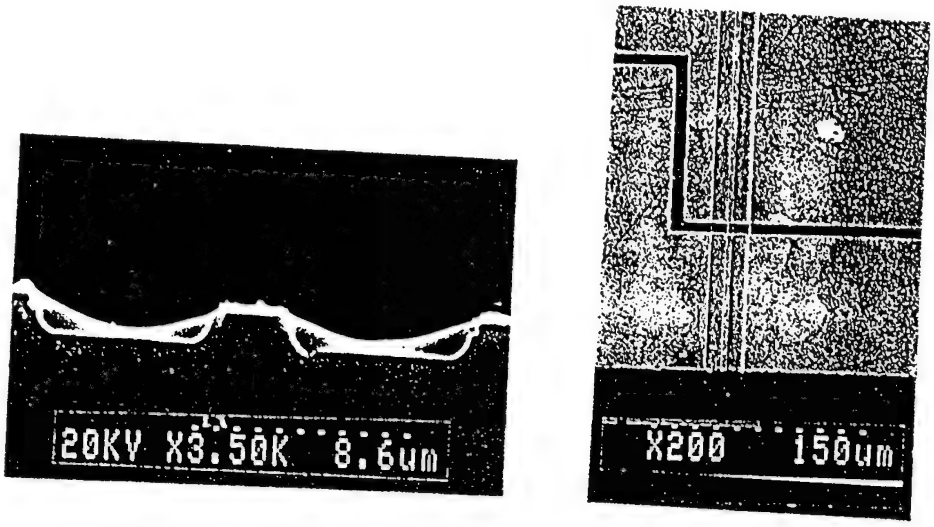

Fig.3.8b. The SEM picture of a ridge waveguide two section laser diode.

3.10. Wafer scribing

Using a good diamond knife and scribing machine, to separate wafers into laser bars. The important points are(Fig.3.9):

1. According to required cavity length, in the direction normal to the waveguide, cut short trace near the edge of the wafer, and then fracture along its crystal structure. This method should reveal perfect facets perpendicular to the waveguide. Never cut the wafer all the way down across its whole area, as the knife tip will definitely damage the facet if the tip touches the ridge.
2. Carefully place the laser bar on stick film and place the film back to scriber, and scribe all the way down along the waveguide direction in order to get separate laser diodes, but the cutting point should be far from the waveguide.

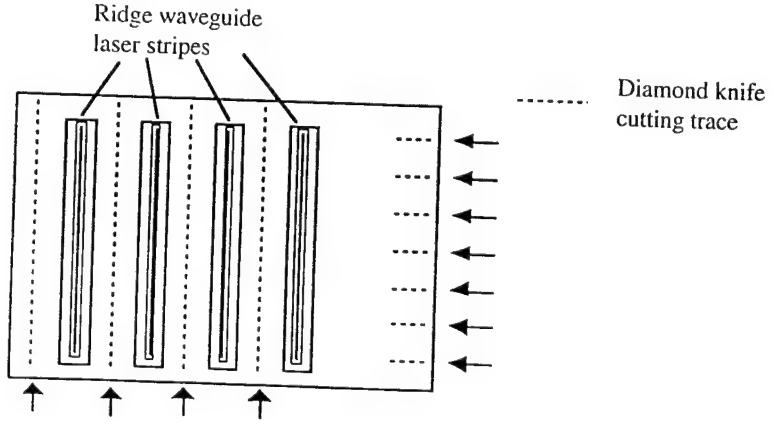

Fig. 3.9. The scribing method is shown for cutting wafer into laser bars and dice.

3.11. Laser diode assembling

Generally, a heat sink is used as the packaging base for mounting laser diodes. The heat sink should be coated with gold for good electric conductivity and long lift-time. Indium is used as the bonding material between the laser chip and the base of the heat sink.

1. Clean sub-mount: use hot TCE→cool TCE→acetone→methanol, plus ultrasonic, to clean the sub-mount(heat sink).
2. Place heat sink on 150 ^{0}C hotplate, and put several 0.005″ indium balls on the base of heat sink. Let the indium melt, then add some flux to keep a good shape of melted indium.
3. Using fine tip tweezers, by NOT touching the waveguide facets of the laser diode, pick up a laser chip carefully and place it at the top of the melted indium.
4. Carefully adjust the chip position on the heat sink. One of the facets should be about 10 μm from the edge of the heat sink, and should be parallel with the edge, as shown in Fig.3.10.

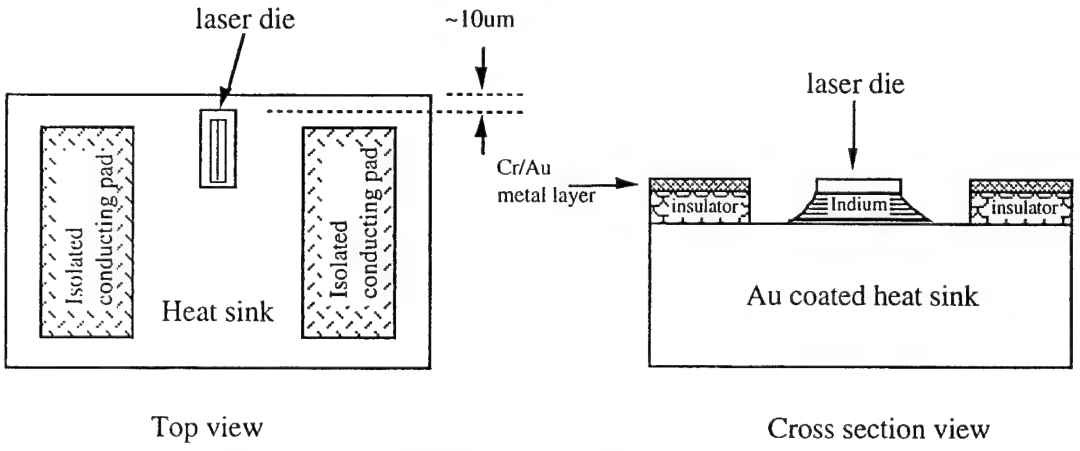

Fig. 3.10. The diagram shown laser die mounting.

5. Remove the heat sink out of the hot plate and allow it to cool. Use the ultrasonic bonding machine to bond Au wire between the top metal contact of the laser chip and the isolated conducting pad of the heat sink.
6. Carefully bond the connecting wire to the conducting pad of the heat sink by iron solder.

Up to now, the processing for laser diode is finished. The Laser diode is ready for electrical and optical tests.

3.12. conclusion

We have presented the laser diode processing method in detail. Apart from good quality of epitaxial growth, wafer processing is also crucial to the performance of a laser diode. Among them, successful metal lift-off, good Ohmic contact and perfect waveguide facets are especially important.

3.13. Reference

1. B. Garrett and R. W. Glew, "Low threshold, high power zero-order lateral mode DQW-SCH metal clad ridge waveguide AlGaAs/GaAs lasers", *Electronics Letters*, **23**(8), 371-373(1987)
2. M. Hatzakis, B. J. Canavello and J. M. Shaw, *IBM J. RES. DEVELOP.*, **24**(4), 452-460(1980)
3. G. G. Collins and C. W. Halsted, *IBM J. RES. DEVELOP.*, **26**, No.5, 596-604(1982)
4. A. Fathimulla, *J. Vac. Sci. Technol.*, B, **B3**(1), 25-27(1985)
5. Y. A. Gol'dberg, "Ohmic metal/III-V semiconductor contact: fabrication methods and properties (review) ", *Semiconductor*, **28**(10), 935-43(1994).

Appendix: Laser Fabrication Masks

Marks Mask: *Mask 3*

Ridge Mask: *Mask 11*

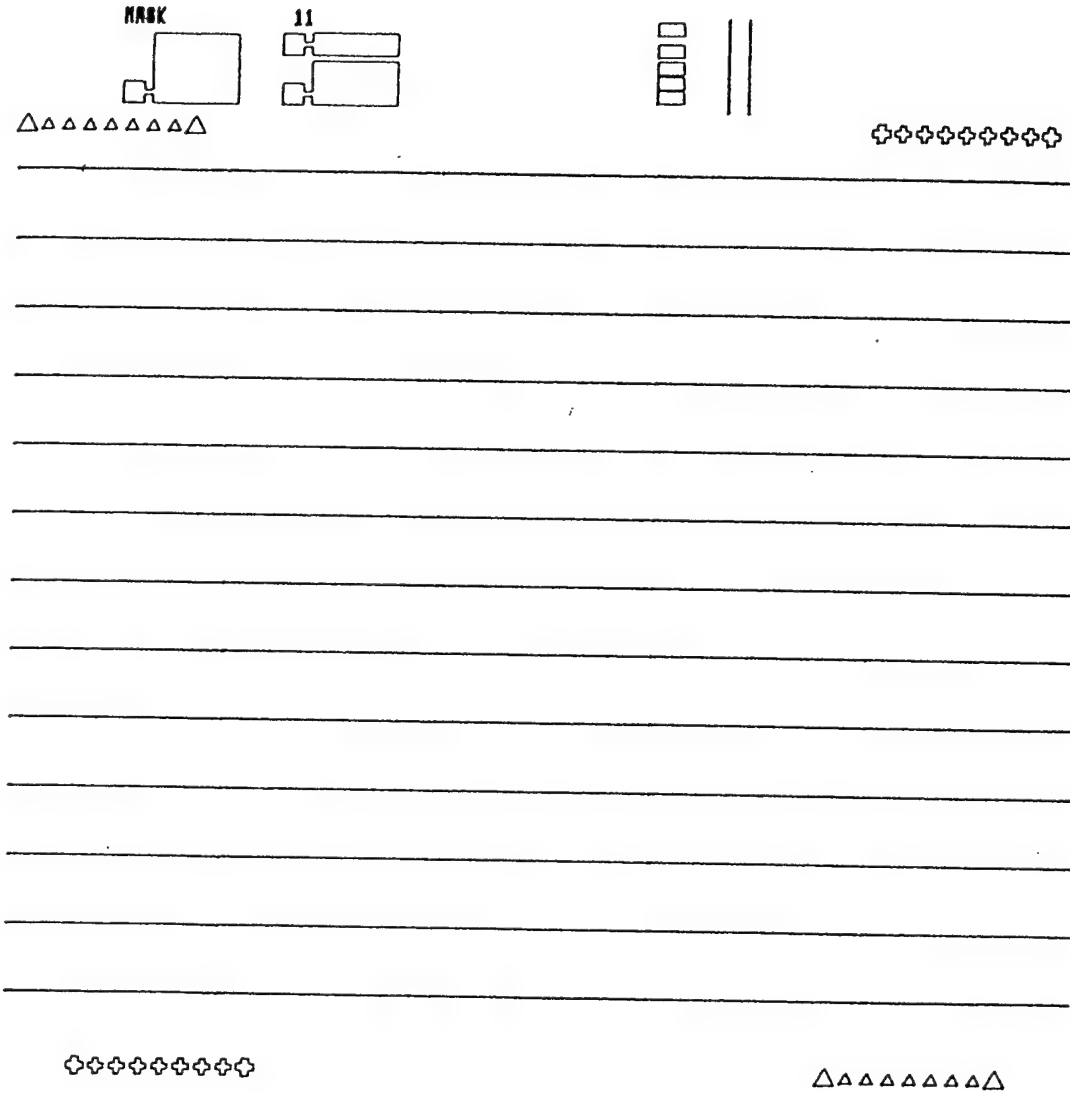

Trough Etch Mask: *Mask 4*

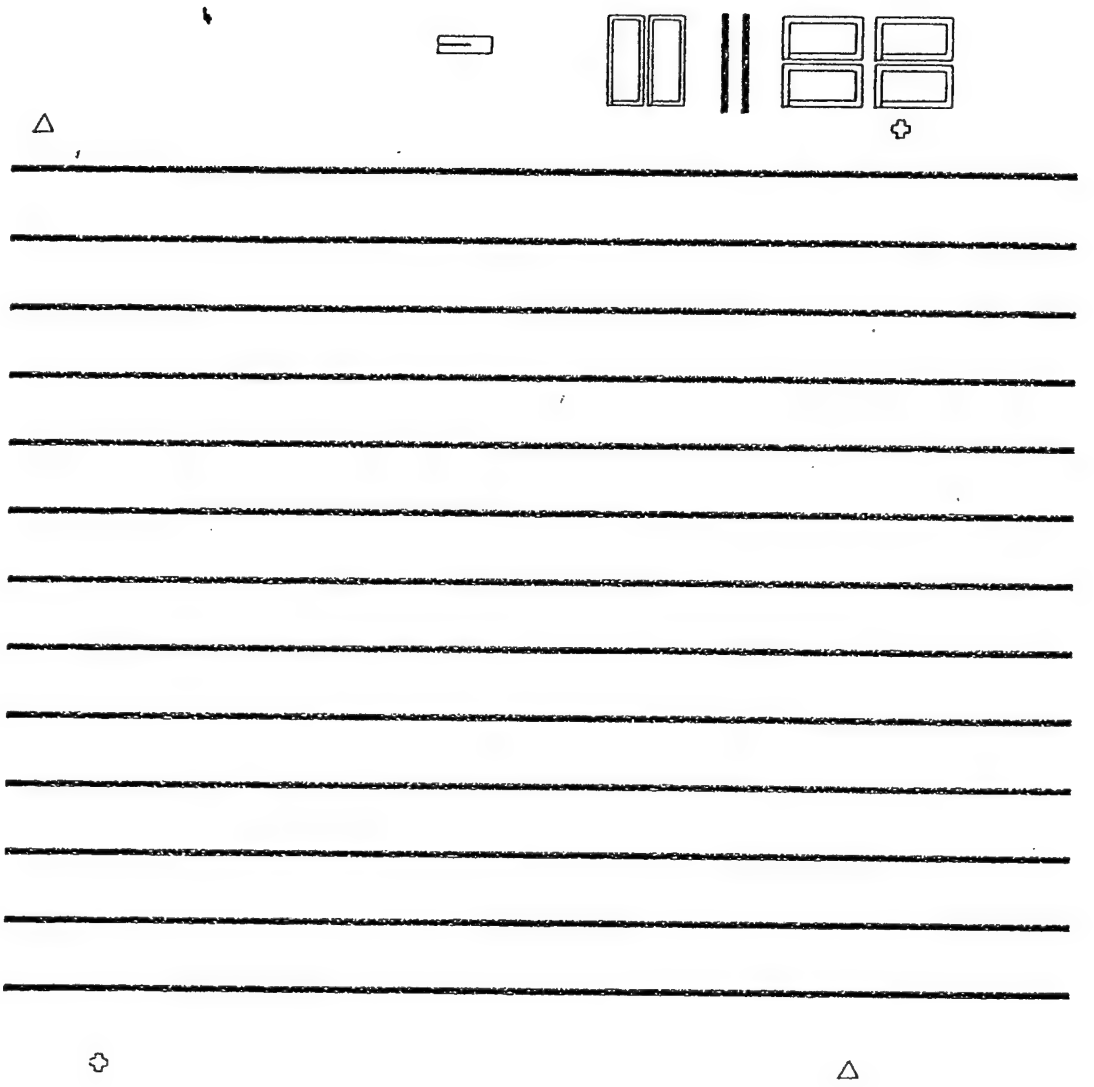

Final Metalisation Mask: *Mask 8*

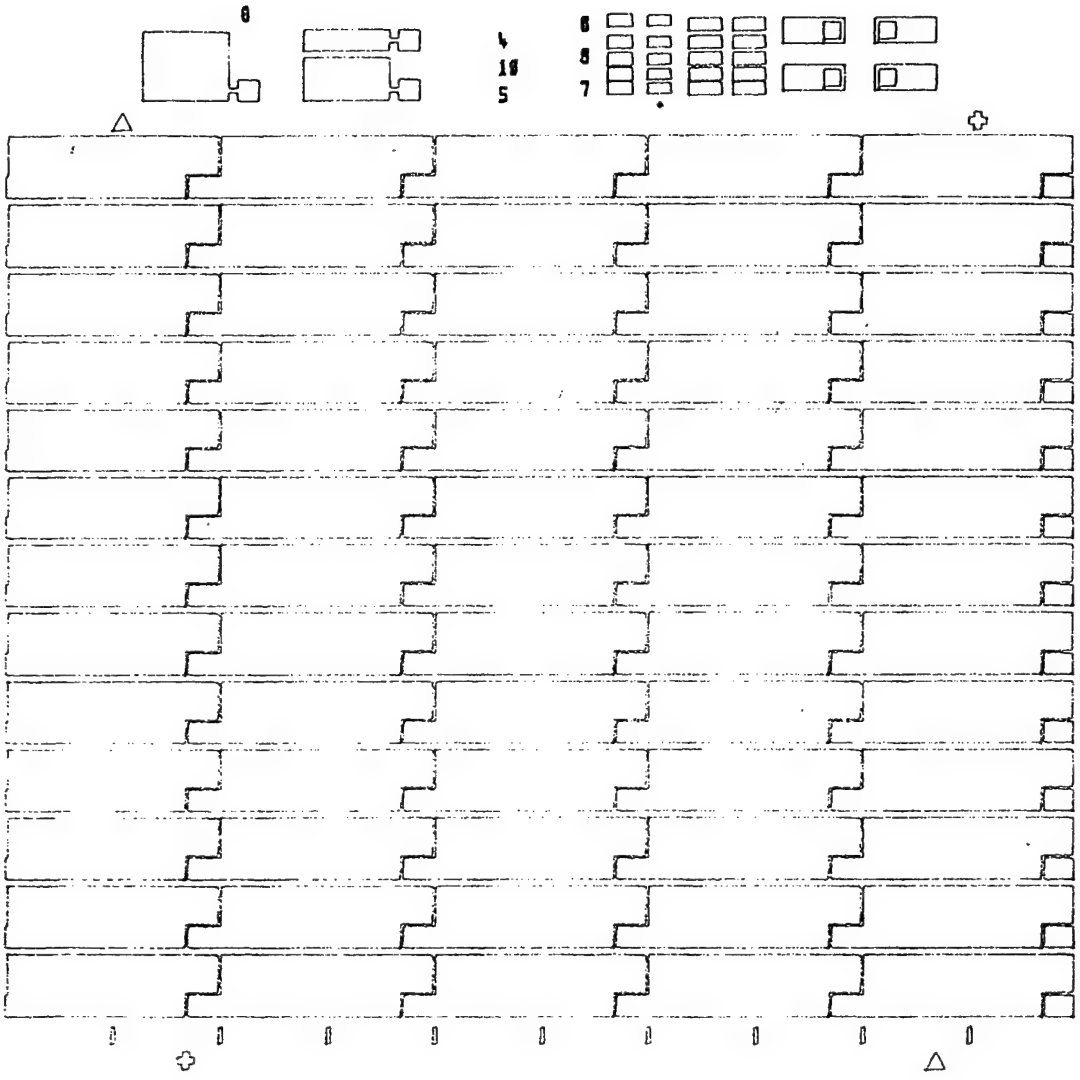

4. Experimental Results

Introduction

For a successful monolithic tunable laser, the first thing is that the device should work as a desired laser. Our first aim was to achieve a CW working, single longitudinal mode ridge waveguide laser with reasonable linewidth.

We have successfully fabricated room temperature CW working lasers in the first few processing runs. In this chapter, we present some test and measurement results we obtained so far. Further tests and measurements are currently underway, whose results will be presented later.

The results we have obtained are mainly related to the electrical and optical performance of our laser diodes, which is an indication of epitaxial growth quality, device design and fabrication processing problems.

4.1. Electrical characteristics

A laser diode is basically a normal semiconductor p-n junction device with large forward current, which is very likely to cause the device temperature to rise. The lasing emission activity is very sensitive to temperature (higher temperature results in higher non-radiation recombination, higher threshold current and lower internal quantum efficiency) and temperature variation (due to thermal effect of refractive index, emission mode and wavelength changes accordingly), a good Ohmic contact device is very important for the laser diodes.

4.1.1. Ohmic contact of the device

For our device, the n-type doping is silicon in the substrate. The most commonly and successfully used contact metals are Ni/AuGe (alloy of 88% Au and 12% Ge, first layer AuGe and second layer Ni) system.[1] In order to have a smoother interface, better surface morphology and stronger adherent to the GaAs surface,[2] we use Au/Ni/AuGe/Ni for our n-type metalisation. For the p-type Zn doping GaAs cap layer, Au/Zn or Pb/Zn are the commonly used metals for contact,[3] but due to the high vapour pressure of Zn which can contaminate vacuum systems and its high diffusivity which can penetrate the contact layer and degrade the active region, we have chosen alternatively Au/Cr and Au/Ti as the contact metals, which are also proved to have low contact resistivity to p-type GaAs[4] and are suitable for use in laser diodes.[5]

(i) Method used for contact resistance measurement

We use the transmission line method (TLM)[6] to measure the contact resistance of our device. It is a simple and widely used method. In this particular approach, a linear array of contacts is fabricated with various spacing between them, as shown in Fig.4.1a. The resistance is measured as a function of the gap spacing (Fig.4.1b), and extrapolation of the resistance to zero gap spacing gives a value equal to $2R_c$, or, the total measured resistance $R_T=2R_c$ (two contacts) + R_b (bulk

resistance of the material), and $R = \rho \ell / A$, where ρ is the average resistivity of the semiconductor layer and A is its cross sectioned area perpendicular to ℓ. When $\ell = 0$, $R_T = 2R_c$.

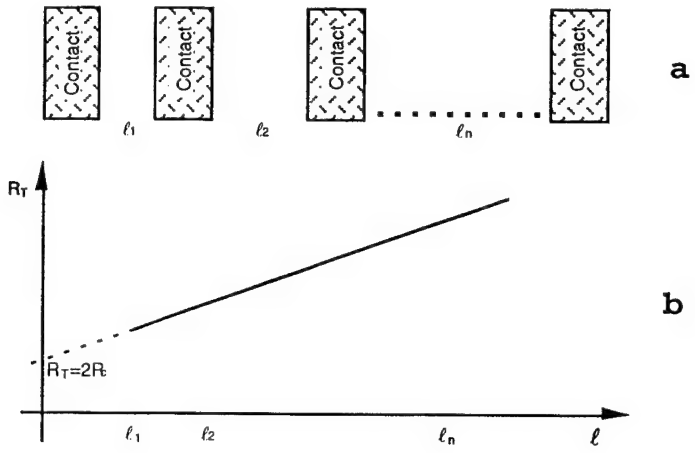

Fig. 4.1 TLM to measure contact resistance.

(ii). Contact resistance measurement results

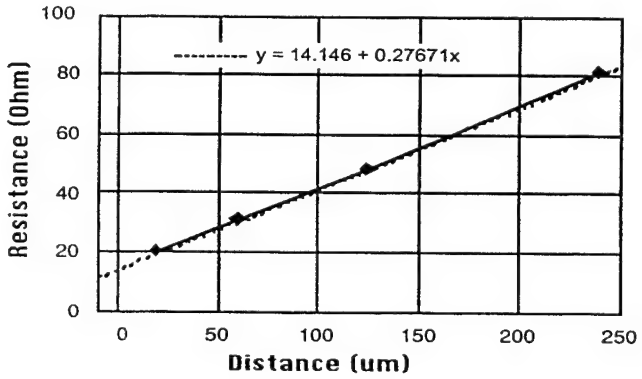

Fig. 4.2 Contact resistance measured by TLM.

Fig.4.2 is a typical experimental result for contact to p-GaAs by using this method. Each contact resistance data is obtained by I-V measurement, as show in Fig.4.3, also shown in the inset is the typical I-V curve which is obviously ohmic in nature. From our measurement, the typical specific contact resistance is about $2X10^{-4}$ $\Omega.cm^2$ for our device, compared to 10^{-6} $\Omega.cm^2$ specific contact resistance, which is the normally achievable and widely reported value in literature[2], what we obtained is certainly not the ideal. Indeed, we occasionally observed non-Ω contact I-V curves during TLM measurements. Some investigation for better metalisation is planned for the next step.

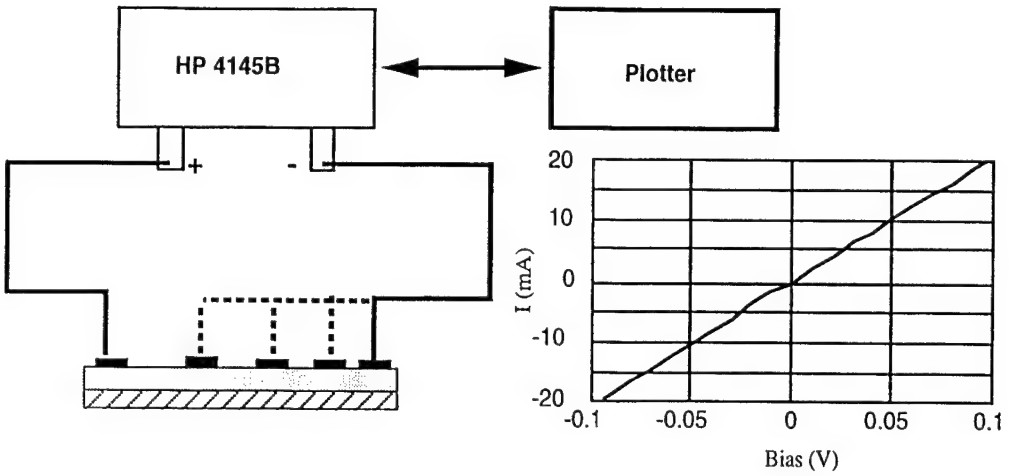

Fig.4.3 The measurement arrangement for contact resistance.
Inset shows the typical I-V curve.

4.1.2. Current-voltage (I-V) characteristics

An ideal p-n junction is important for the good performance of a laser diode. Under forward bias, the I-V characteristics of an ideal laser diode is dominated by carrier diffusion and recombination processes, but for a practical device, due to inevitable contact resistance and series resistance, the I-V characteristics is dominated by the Ohmic nature (linear relation between current and voltage) instead of exponential characteristics at high injection current. The slope at the high current injection region is a good estimate of the contact and series resistance of the device. Under reverse bias, the leakage current is very small until the break down voltage, but for a non-ideal diode, the leakage current increases with the reverse bias due to the imperfect p-n junction and surface leakage. For a laser diode, a totally "soft" reverse biased I-V curve means the exiting of serious current leakage such that an important part of the current may also be consumed due to this leakage even under forward bias, which means the desired carrier confinement in the active layer is seriously degraded and the diode may fail to lase.

Fig.4.4 is the experimental arrangement for I-V characterisation. Fig.4.5 shows the typical I-V characteristics of our laser diode and the I-V curve of a commercial laser diode made by BNR which has quite similar epitaxy structure to our device except lower Al composition in its cladding and barrier layers[7]. They both are mounted and bonded under the same conditions. From the comparison we see quite similar characteristics, and the turning point in our device is at higher voltage, which is partly due to higher Al composition in our structure, and partly due to the non-ideal contact. From the obviously different slopes of these two curves, we conclude that the total resistance in our device is larger than that of the BNR laser. Fig.4.6 shows the I-V curves for estimating the contact and series resistance and its value from the slope. Indeed, our device shows larger resistance, which confirms that a further improvement in our device contact is necessary.

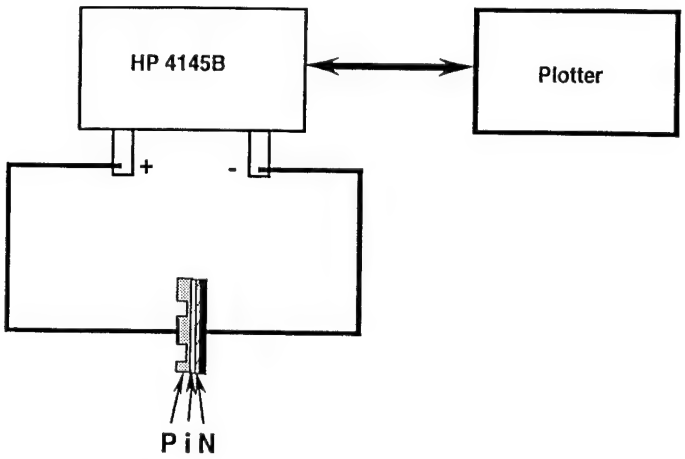

Fig.4.4 I-V measurement set-up.

4.2. Optical characteristics

For a laser diode, the most important characteristic is its optical performance, such as optical power-driving current (L-I) characteristics, spectrum and the linewidth. From these measurements, we obtain information about the cavity loss, mode behaviour in the designed waveguide and more generally, the quality of the epitaxial growth and the fabrication process. All this information is important for modification and improvement to the design and fabrication process.

The measurements are performed at room temperature, and the laser is run in CW operation. The laser sub-mount is placed on a Peltier cooler/heater with an embedded thermistor inside it to enable its temperature to be controlled by a electronic controller. All lasers are the natural crystal facet with no AR or reflective coating.

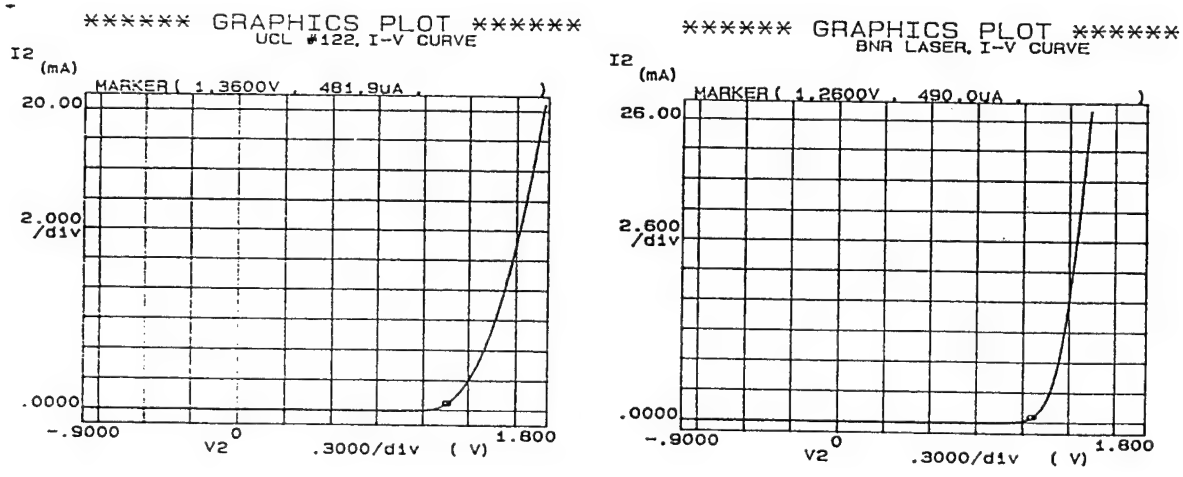

Fig.4.5 Measured I-V curve and comparison to BNR laser.

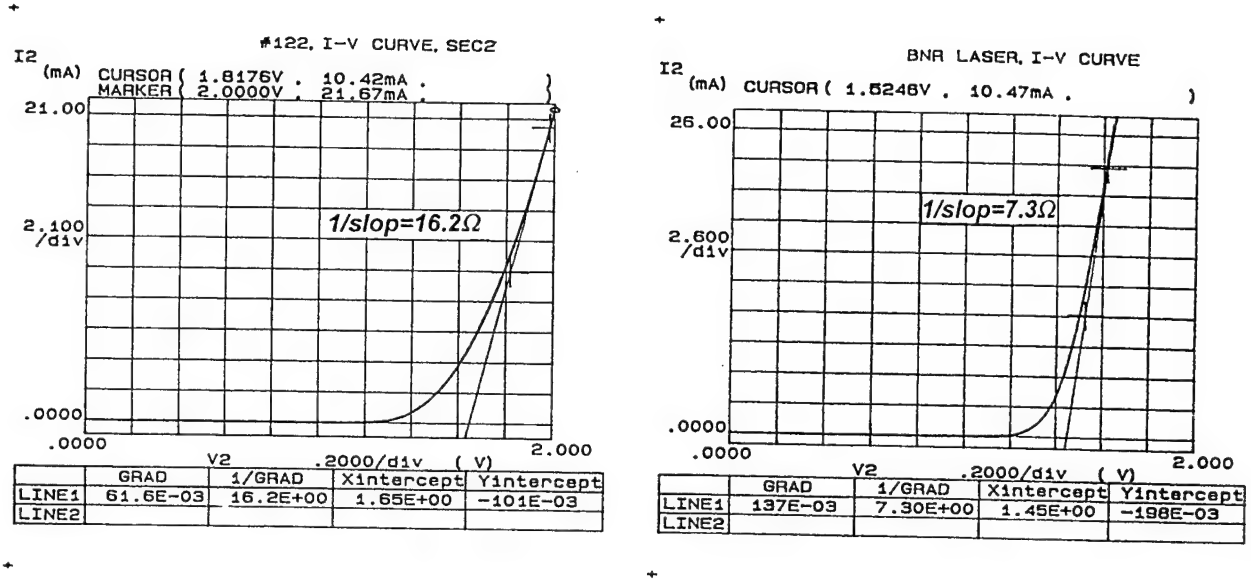

Fig.4.6 Estimating total resistance from the slopes at high current injection region of measured I-V curves.

4.2.1. The measurement of L-I curve

Fig.4.7 is the measurement arrangement for L-I characteristics. The measurement is carried out under CW operation and at room temperature and the laser diode sub-mount is temperature controlled at around 18 °C. Fig.4.8 shows typical results of this measurement. The threshold current is approximately 25 mA for the 300-500 μm cavity lasers.

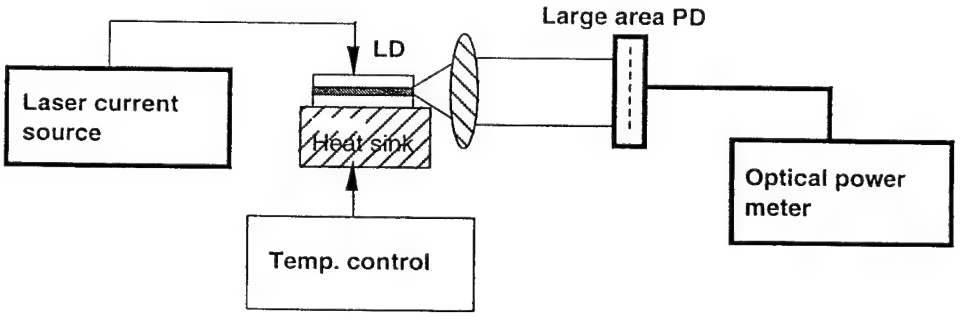

Fig.4.7. Schematic diagram for L - I measurement.

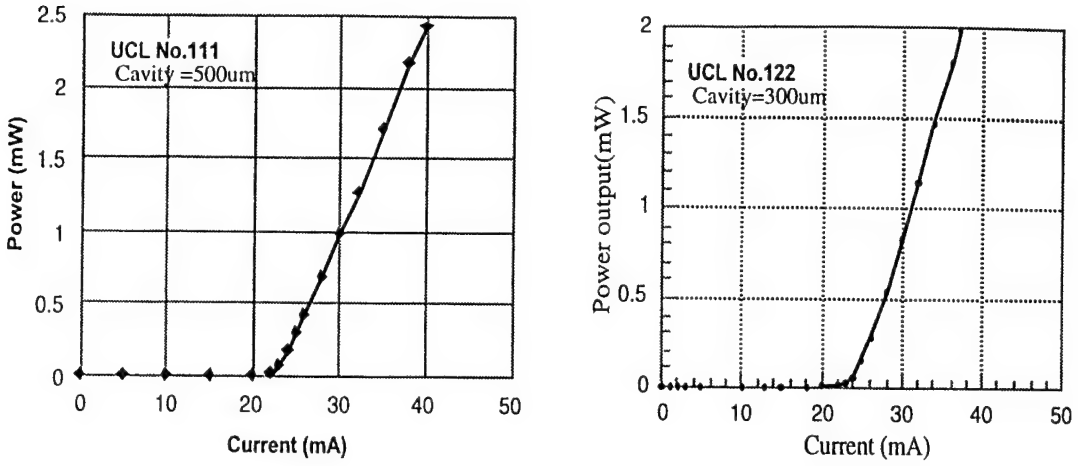

Fig.4.8 CW operation light power output versus current curves for some lasers.

The slope efficiency is approximately 0.1-0.2 mW/mA, and the maximum output power per facet is 10 mW which is lower than normally reported results from literature.[7,8] We realise this is due to the high contact resistance which is confirmed by electrical measurement, and the high cavity loss which is confirmed by independent analysis performed on the same epitaxy wafer by Sheffield. Their test and measurement on the quality of the epitaxy growth confirms that due to oxygen contamination during growth, the oxygen concentration in the epitaxial layer is higher than allowed, resulting in a large non-radiation centre in the MQW active layer, therefore, reducing the internal quantum efficiency and increasing the cavity loss. Further improving the epitaxial growth quality is planned, including to degas the reactor chamber and change the MOVPE source. Upon completion of improvements, our laser should have higher internal quantum efficiency and lower loss. Much higher output power should be achievable.

4.2.2. Spectrum characteristics

Some important information, such as lasing wavelength, mode behaviour and side mode suppression , could be obtained from laser spectrum analysis. Fig. 4.9 is the arrangement for spectrum measurement. Caution has been made to avoid the optical feedback from different optical elements. Fig.4.10 is the typical spectrum under different driving currents. When current is higher than $1.5I_{th}$, the spectrum becomes single mode dominated with mode suppression ratio (MSR) larger than 15dB. After $I > 44$mA, the MSR remains at almost 20dB with no mode jumping up to I=56 mA. The wide single mode working current range is certainly not too bad in comparison with some reported results with a similar laser structure.[9] Since in our study, the purpose is not to achieve a high value of MSR, the 20 dB side mode suppression is reasonably good for our study on reverse bias tuning. Further improvement is possible through improving internal quantum efficiency, therefore increasing the central mode power.

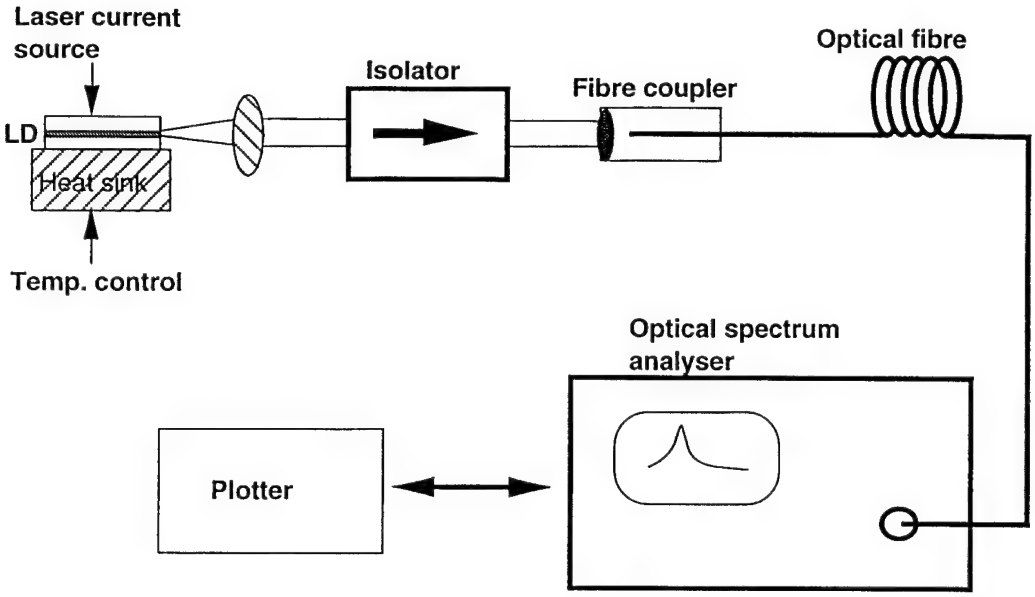

Fig.4.9 Schematic diagram for optical spectrum measurement.

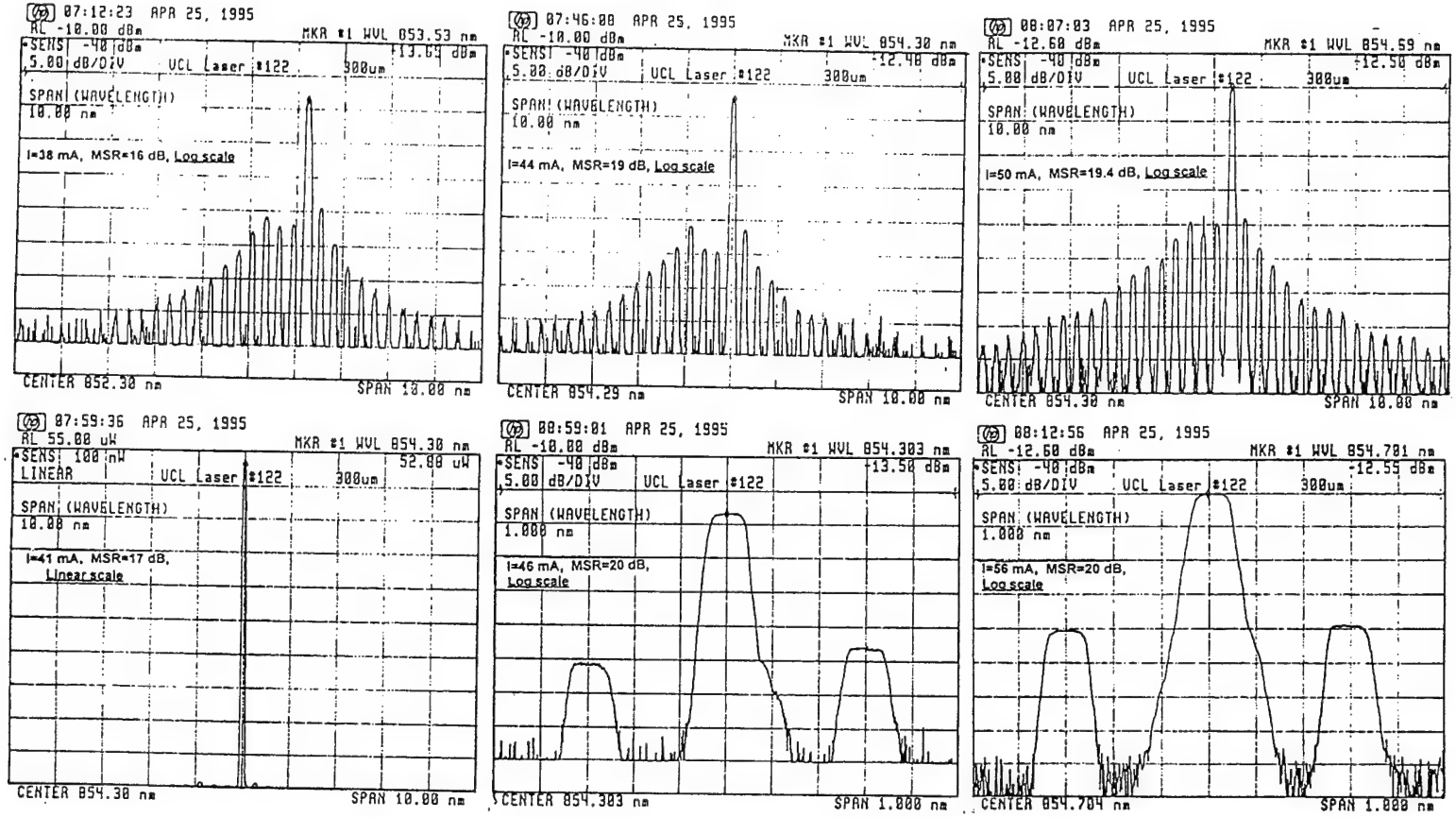

Fig.4.10 Lasing spectrum under different pump current. CW operation, 18C.

4.2.3. Linewidth measurement

Apart from optical spectrum, laser emission linewidth is also an important parameter of concern. Fig.4.11 is the schematic diagram for our delayed self-homodyne linewidth measuring system.[10,11] Fig.4.12 is the measured result for I=45 mA. The linewidth of over 70MHz, compared to about 2.5MHz measured from a BNR laser which has a similar structure but with one facet AR coated, is a clear indication that there exists a large internal loss mechanism . Indeed, the maximum output power of our laser is about five times lower than that of the BNR laser. On improving the epitaxial growth and our fabrication process, reducing the linewidth to below 20 MHz should not be too difficult, and will fulfil our requirement for carrying out our study on reverse biased tuning.

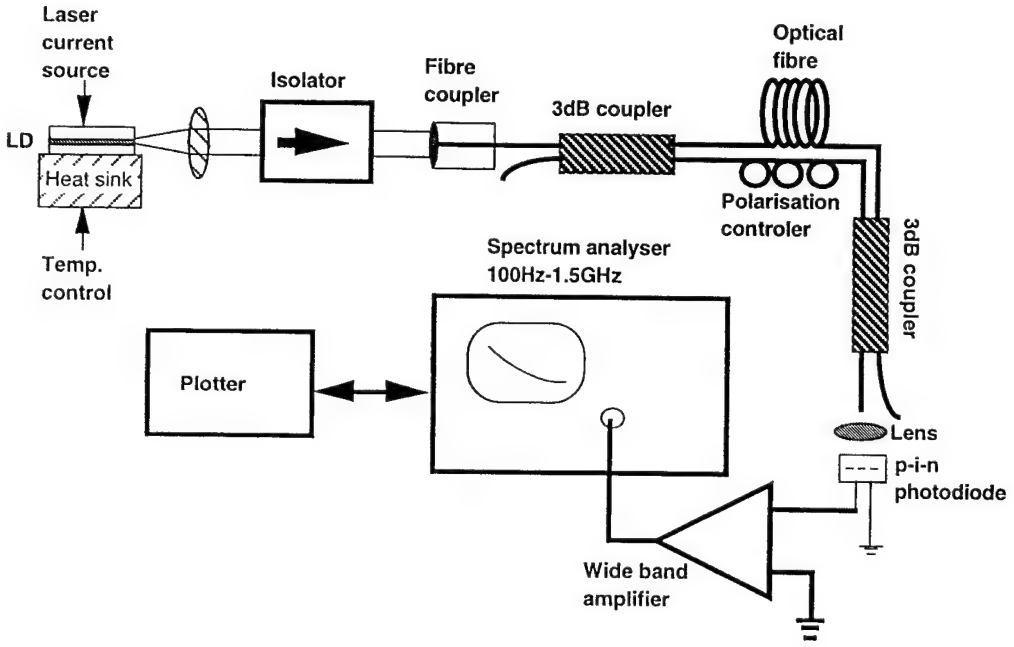

Fig.4.11 Schematic diagram of delayed self-homodyne linewidth measurement for laer diodes.

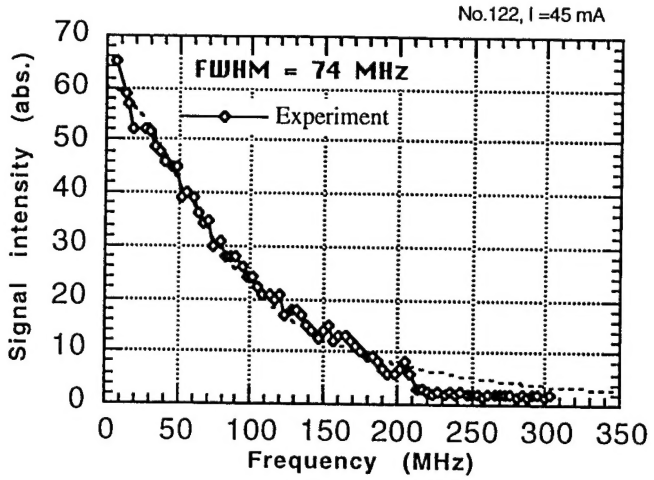

Fig.4.12. The linewidth measurement result.
Dashed line is the Lorenzian curve fitting result.

In conclusion, our experimental results show that we have successfully fabricated CW working, single longitudinal mode MQW lasers, making our attempt to study two section, reverse biased tunable lasers by using QCSE as the tuning mechanism become a reality. Large contact resistance, poor internal quantum efficiency and large cavity loss are found from these measurements. With further improvement on structure growth, contact and other fabrication techniques, further improvement on the laser performance, including increase of MSR and decrease of linewidth, should be possible.

4.3. Reference

1. N. Braslau, *J. Vac. Sci. Technol., A*, **4**, 3058(1986).
2. T. C. Shen, G. B. Gao and H. Horkoc, "Recent developments in ohmic contacts for III-V compound semiconductors", *J. Vac. Sci. Technol., B*, **10**(5), 2113-32(1992).
3. Y. C. Lu, T. S. Kalkur and C. A. Paz de Araujo, *J. Electrochem. Soc.*, **136**, 3123(1989).
4. R. Castanedo, R. Asomoza, G. Jimenez, S. Romero and J. L. Pena, "Contact resistivity and SIMS-Auger analysis of Au/Cr contact on p-GaAs", *J. Vac. Sci. Technol., A*, **4**(3), 814-7(1986).

   R. P. Gupta and J. Freyer, "Metalisation systems for ohmic contacts to p- and n-type GaAs", *Int. J. Electronics*, **47**(5), 459-67(1979).
5. R. W Glew, B. Garrett, J. E. A. Whiteway and E. J. Thrush, "GaAs/GaAlAs LOC lasers grown by MOCVD", *J. Cryst. Growth*, **77**, 613-20(1986).
6. V. L. Rideout, *Solid-State Electron.* **18**, 541(1975).
7. I. B. Garrett and R. W. Glew, "Low threshold, high power zero-order lateral mode DQW-SCH metal clad ridge waveguide AlGaAs/GaAs lasers", *Electronics Letters*, **23**(8), 371-373(1987)

8. M. Hung, K. Din, C. Chen, C. Chang and B. Lee, "Ridge waveguide modified triple quantum well high power AlGaAs laser grown by MOVPE", *SPIE* **Vol. 1813**, *Optoelectronic Component Technologies*, 27-32(1992).
9. B. Garrett, I. H. White and D. F. G. Gallagher, "Self longitudinal mode stabilisation in GaAs/AlGaAs quantum well lasers", *Electronics Letters*, **23**(22), 1193-4(1987)
10. K. Iiyama, K. Hayashi, Y. Ida, S. Tabata and Y. Sakai, "Delayed self-homodyne method using solitary monomode fibre for laser linewidth measurements", *Electron. Lett.*, **25**(23), 1589-90(1989).
11. I. W. Oh and H.R.D. Sunak, "Measurement of the spectral linewidth of semiconductor lasers for use with coherent optical communication systems", *IEEE Trans. on Instrumentation and Measurement*, **IM-36**(4), 1054-1059(1987)

5. Further Work

Introduction

In the first year of work we have successfully designed and fabricated a two contact ridge guide MQW laser capable of room temperature CW operation in a single longitudinal mode, with the excellent threshold current of about 25 mA. This provides a firm foundation for the remainder of our programme on QCSE tuned semiconductor lasers. Our further work is conveniently divided into:(1) Device processing and device design development; (2) Device and material characterisation; (3) Ion implantation to achieve isolation;(4) Tuning section band gap shift; and (5) Further tuning consideration.

5.1 Device Processing and Device Design Development

Throughout this first year of the work the importance of suitable contacting processes to avoid thermal artefacts obscuring CW device behaviour has been emphasised. We aim to carry out a more systematic study of contacting processes to determine an optimum metallisation scheme for our requirements.

Some modification of the mask set will be necessary in order to reduce parasitic capacitance and thus increase the cut-off frequency, if the ultimate limits of the tuning technique are to be explored. Both air bridge and polyimide techniques will be considered for this purpose. Isolation between gain and tuning sections using guard contact techniques will also be considered.

5.2 Device and Material Characterisation

More characterisation of laser diodes and later, tunable lasers will be carried out including quantum efficiency, near and far field pattern, isolation effects, IFVD blue shift, tuning response and speed, optical FM spectrum and dynamic side-mode suppression. In the second year of the work we expect to make the first measurements of QCSE tuning in the monolithic structure.

Device characterisation will be supported by QCSE material characterisation, including the fabrication of normal incidence structures for detailed material assessment.

5.3 Ion Implantation for Electrical Isolation

The first experimental run of the process is already under way. This experiment is in collaboration with the EPSRC Ion Implantation Centre at the University of Surrey. We choose O^+ and RTA annealing as the method for electrical isolation in this experiment. Proton bombardment is also going to be used in a comparitive study of electrical and optical characteristics. Measurement on the

isolation resistivity and the optical loss in the implanted region will be completed in the second year of our work.

5.4 Band Gap Shift in Tuning Section

The IFVD technique is going to be used as the method to optimise the exciton wavelength in the tuning section. This will involve a collaboration with the EPSRC III-V Semiconductor Facility at the University of Sheffield. Combined with the experimental measurement of tuning characteristics, we will determine the operation wavelength and the corresponding refractive index change in the tuning section. Photo-luminescence (PL) will be used as the tool to check the band gap shift resulting from RTA processing of the capped areas, before laser fabrication.

5.5 Further Consideration of Tuning using QCSE

The large absorption at the wavelength of maximum refractive index change is a disadvantage of the QCSE tuning mechanism. There is a possible method to tailor this characteristics through band gap engineering, to achieve large refractive index change and maintain lower absorption.[1,2]. It will be interesting to investigate the possibility of applying this technique to our laser structures.

5.6 Conclusion

In this report we have chosen that QCSE is a highly attractive tuning technique for semiconductor lasers, offering flat FM frequency response into the millimetre-wave region, in relatively simple laser structures. In the first year of this project, supported under the Special Contract, we have met our stated goals of designing and fabricating a monolithic semiconductor laser capable of demonstrating the technique and have demonstrated room temperature CW single mode operation of the laser.

We now go forward to explore isolation and IFVD quantum well modification techniques techniques leading to demonstration of the reverse bias tuning characteristics of the device.

5.7 Reference

1. W. Batty and D. W. E. Allsop, "Low voltage, high bandwidth optical modulation utilising enhanced electrorefractive effects in shaped quantum wells", *SPIE* **Vol.2212**, 106-117(1994).
2. W. Batty and D. W. E. Allsop, "Internal biasing by -doping for low voltage, high bandwidth quantum well optical modulators", *IEEE Photon. Technol. Lett.*, **7**, June (1995).